



**HAL**  
open science

## Repression of SATB1 in regulatory T cells is required for suppressive function and inhibition of effector differentiation

Joachim L Schultze, Marc Beyer, Yasser Thabet, Sabine Classen, Eva Schoenfeld, Andrea Gaarz, Svenja Debey-Pascher, Roman U. Mueller, Bernhard Schermer, Timothy Sadlon, et al.

### ► To cite this version:

Joachim L Schultze, Marc Beyer, Yasser Thabet, Sabine Classen, Eva Schoenfeld, et al.. Repression of SATB1 in regulatory T cells is required for suppressive function and inhibition of effector differentiation. *Nature Immunology*, 2011, 10.1038/ni.2084. hal-00669816

**HAL Id: hal-00669816**

**<https://hal.science/hal-00669816>**

Submitted on 14 Feb 2012

**HAL** is a multi-disciplinary open access archive for the deposit and dissemination of scientific research documents, whether they are published or not. The documents may come from teaching and research institutions in France or abroad, or from public or private research centers.

L'archive ouverte pluridisciplinaire **HAL**, est destinée au dépôt et à la diffusion de documents scientifiques de niveau recherche, publiés ou non, émanant des établissements d'enseignement et de recherche français ou étrangers, des laboratoires publics ou privés.

# Repression of SATB1 in regulatory T cells is required for suppressive function and inhibition of effector differentiation

Marc Beyer<sup>1</sup>, Yasser Thabet<sup>1</sup>, Roman-Ulrich Müller<sup>2,3</sup>, Timothy Sadlon<sup>4</sup>, Sabine Classen<sup>1</sup>, Katharina Lahl<sup>5</sup>, Samik Basu<sup>6</sup>, Xuyu Zhou<sup>7</sup>, Samantha L. Bailey-Bucktrout<sup>7</sup>, Wolfgang Krebs<sup>1</sup>, Eva A. Schönfeld<sup>1</sup>, Jan Böttcher<sup>8</sup>, Tatiana Golovina<sup>6</sup>, Christian T. Mayer<sup>5</sup>, Andrea Hofmann<sup>1</sup>, Daniel Sommer<sup>1</sup>, Svenja Debey-Pascher<sup>1</sup>, Elmar Endl<sup>8</sup>, Andreas Limmer<sup>8</sup>, Keli L. Hippen<sup>9</sup>, Bruce R. Blazar<sup>9</sup>, Robert Balderas<sup>10</sup>, Thomas Quast<sup>11</sup>, Andreas Waha<sup>12</sup>, Günter Mayer<sup>13</sup>, Michael Famulok<sup>13</sup>, Percy A. Knolle<sup>8</sup>, Claudia Wickenhauser<sup>14</sup>, Waldemar Kolanus<sup>11</sup>, Bernhard Schermer<sup>2,3</sup>, Jeffrey A. Bluestone<sup>7</sup>, Simon C. Barry<sup>4</sup>, Tim Sparwasser<sup>5</sup>, James L. Riley<sup>6</sup>, Joachim L. Schultze<sup>1</sup>

<sup>1</sup> *LIMES-Institute, Laboratory for Genomics and Immunoregulation, University of Bonn, Carl-Troll-Str. 31, 53115 Bonn, Germany*

<sup>2</sup> *Renal Division, Department of Medicine and Centre for Molecular Medicine, University of Cologne, Kerpener Str. 62, 50937 Cologne, Germany*

<sup>3</sup> *Cologne Excellence Cluster on Cellular Stress Responses in Aging-Associated Diseases, University of Cologne, Zùlpicher Strasse 47a, 50674 Cologne, Germany*

<sup>4</sup> *Discipline of Paediatrics, Women's and Children's Health Research Institute, University of Adelaide, 72 King William Road, North Adelaide, 5006, Australia*

<sup>5</sup> *Institute of Infection Immunology, TWINCORE, Centre for Experimental and Clinical Infection Research, a joint venture between the Medical School Hannover (MHH) and the Helmholtz Centre for Infection Research (HZI), Feodor-Lynen-Str. 7, 30625 Hannover, Germany*

<sup>6</sup> *Department of Microbiology, Translational Research Program, Abramson Family Cancer Research Institute, University of Pennsylvania, Room 556 BRB II/III, 421 Curie Blvd., Philadelphia, PA 19104-6160, USA*

<sup>7</sup> *Diabetes Center and the Department of Medicine, University of California, 513 Parnassus Avenue, Box 0540, San Francisco, CA 94143, USA.*

<sup>8</sup> *Institutes of Molecular Medicine and Experimental Immunology, University Hospital Bonn, Sigmund-Freud-Str. 25, 53105 Bonn, Germany*

<sup>9</sup> *Cancer Center and Department of Pediatrics, Division of Blood and Marrow Transplantation, University of Minnesota, Mayo Mail Code 109, 420 Delaware St. SE, Minneapolis, MN 55455, USA*

<sup>10</sup> *BD Biosciences – Pharmingen, 10975 Torreyana Road, San Diego, CA 92121, USA*

<sup>11</sup> *LIMES-Institute, Laboratory for Molecular Immunology, University of Bonn, Carl-Troll-Str. 31, 53115 Bonn, Germany*

<sup>12</sup> *Department of Neuropathology, University Hospital Bonn, Sigmund-Freud-Str. 25, 53105 Bonn, Germany*

<sup>13</sup> *LIMES-Institute, Laboratory of Chemical Biology, University of Bonn, Gerhard-Domagk-Str. 1, 53121 Bonn, Germany*

<sup>14</sup> *Department for Diagnostic, Institute for Pathology, University Hospital Leipzig, Liebigstr. 26, 04103 Leipzig, Germany*

**Correspondence should be addressed to J.L.S. ([j.schultze@uni-bonn.de](mailto:j.schultze@uni-bonn.de)).**

**Regulatory T (T<sub>reg</sub>) cells are essential for self-tolerance and immune homeostasis. Lack of effector T cell (T<sub>eff</sub>) function and gain of suppressive activity by T<sub>reg</sub> are dependent on the transcriptional program induced by Foxp3. Here we report repression of SATB1, a genome organizer regulating chromatin structure and gene expression, as crucial for T<sub>reg</sub> phenotype and function. Foxp3, acting as a transcriptional repressor, directly suppressed the *SATB1* locus and indirectly through induction of microRNAs that bound the *SATB1* 3'UTR. Release of *SATB1* from Foxp3 control in T<sub>reg</sub> caused loss of suppressive function, establishment of transcriptional T<sub>eff</sub> programs and induction of T<sub>eff</sub> cytokines. These data support that inhibition of SATB1-mediated modulation of global chromatin remodelling is pivotal for maintaining T<sub>reg</sub> functionality.**

Regulatory T cells ( $T_{\text{reg}}$ ) are characterized by their suppressive function and inability to produce effector cytokines upon activation<sup>1</sup>. Expression of the X-linked forkhead transcription factor Foxp3 has been clearly linked to the establishment and maintenance of  $T_{\text{reg}}$  lineage, identity and suppressor function<sup>2-7</sup>. Moreover, Foxp3 is also associated with the control of effector T cell ( $T_{\text{eff}}$ ) function in  $T_{\text{reg}}$ <sup>4,5</sup>. A growing body of evidence points towards plasticity amongst committed  $CD4^+$  T cell lineages, including  $T_{\text{reg}}$ <sup>8-11</sup>, yet the mechanism for this plasticity and its significance in normal immune responses and disease states remains to be elucidated.

Multiple transgenic reporter mouse models have demonstrated that loss of Foxp3 can induce the conversion of  $T_{\text{reg}}$  into cells with a variety of  $T_{\text{eff}}$  programs<sup>2-4,12</sup>. While  $T_{\text{reg}}$  are re-programmed by loss of the lineage-associated transcription factor Foxp3, there is no evidence that conventional T cells ( $T_{\text{conv}}$ ) actively suppress the  $T_{\text{reg}}$  lineage program. On the contrary, only stable expression of Foxp3 in  $T_{\text{conv}}$  appears capable of inducing a  $T_{\text{reg}}$  phenotype within these cells<sup>7</sup>. Together these findings suggest that  $T_{\text{eff}}$  programs are the default state in  $CD4^+$  T cells and that transcriptional programs induced and maintained by Foxp3 overrule  $T_{\text{eff}}$  function in  $T_{\text{reg}}$ <sup>5</sup>. Whether the inhibition of  $T_{\text{eff}}$  differentiation in  $T_{\text{reg}}$  is critical for  $T_{\text{reg}}$  suppressive function is unclear. Such a model would be supported by the existence of Foxp3-induced mechanisms that continuously and actively control  $T_{\text{eff}}$  programs in these specialized T cells.

Consistent with the active suppression of  $T_{\text{eff}}$  programs in  $T_{\text{reg}}$  cells, ablation of the transcriptional repressor Eos<sup>13</sup> or the Foxo transcription factors<sup>14,15</sup> impart partial  $T_{\text{eff}}$  characteristics to  $T_{\text{reg}}$  cells. Other transcription factors including IRF4 (ref. 16) and STAT3 (ref. 17) have been implicated in the modulation of effector cell differentiation by  $T_{\text{reg}}$  cells<sup>18</sup>. There is evidence that epigenetic control as well as miRNA are important for

Foxp3-mediated suppressive functions<sup>16,19-23</sup>, raising the possibility that epigenetic and post-transcriptional regulation may also be involved in the repression of T<sub>eff</sub> functions in T<sub>reg</sub> cells. These findings support the existence of active regulatory mechanisms that enable committed T<sub>reg</sub> to suppress T<sub>eff</sub> differentiation<sup>24</sup>.

In this report, we specifically searched for genes repressed by Foxp3 in T<sub>reg</sub> that might be central to maintaining regulatory function and suppression of T<sub>eff</sub> function in T<sub>reg</sub> cells. We identified the gene encoding special AT-rich sequence-binding protein-1 (SATB1) to be amongst the most significantly repressed genes in human and murine T<sub>reg</sub> cells. SATB1 is a chromatin organizer and transcription factor essential for controlling a large number of genes participating in T cell development and activation<sup>25</sup>. SATB1 regulates gene expression by directly recruiting chromatin modifying factors to its target gene loci which are tethered to the SATB1 regulatory network through specialized genomic sequences called base-unpairing regions<sup>26,27,28</sup>. In murine T<sub>H2</sub> clones, SATB1 has been shown to function as a global transcriptional regulator specifically anchoring the looped topology of the T<sub>H2</sub> cytokine locus, a pre-requisite for the induction of T<sub>H2</sub> cytokines<sup>29</sup>. Since SATB1-deficient thymocytes do not develop beyond the double-positive stage<sup>25,26</sup>, the role of SATB1 in peripheral T cells, particularly in T<sub>reg</sub>, is still elusive. Repression was mediated directly by transcriptional control of Foxp3 at the *SATB1* locus, **by maintaining a repressive chromatin state at this locus**, and indirectly by Foxp3-dependent miRNAs. Release of *SATB1* from Foxp3 control was sufficient to reprogram natural Foxp3<sup>+</sup> T<sub>reg</sub> into T<sub>eff</sub> cells that lost suppressive function and gained T<sub>eff</sub> function. These findings show that *SATB1* control by Foxp3 is an essential and critical mechanism maintaining T<sub>reg</sub> cell functionality.

## RESULTS

### Human T<sub>reg</sub> cells express low amounts of SATB1

To identify regulatory circuits actively suppressed by Foxp3 as a prerequisite for T<sub>reg</sub> function and inhibition of T<sub>eff</sub> programs, whole transcriptome analysis of human resting or activated T<sub>conv</sub> and natural T<sub>reg</sub> was performed (**Supplementary Fig. 1** and **Supplementary Table 1**). We identified SATB1 as of the 22 genes displaying significant lower expression in T<sub>reg</sub> compared to T<sub>conv</sub> (**Fig. 1a**). Reassessment of transcriptome data from previous reports confirmed our observation of *Satb1* to be a potential target of Foxp3-mediated repression<sup>30-32</sup>.

Transcriptome data were validated in an independent set of samples by qRT-PCR (**Fig. 1b**), immunoblotting (**Fig. 1c**), and single cell analysis by flow cytometry (**Fig. 1d**) clearly demonstrating reduced SATB1 expression in human T<sub>reg</sub>. As increased SATB1 expression has been previously linked to activation of pan-T cell populations<sup>29,33</sup>, we assessed the dynamics of SATB1 protein expression in T<sub>conv</sub> and T<sub>reg</sub> during activation using T cell receptor stimulation in the presence of co-stimulation or interleukin-2 (IL-2) (**Fig. 1e**) as well as mitogens (data not shown). Analysis of SATB1 expression established a stimulation dependent up-regulation of SATB1 in T<sub>conv</sub> while resting T<sub>reg</sub> had a significantly lower SATB1 expression than T<sub>conv</sub> and this expression was only modestly up-regulated after T cell activation. Next we assessed SATB1 in induced T<sub>reg</sub> (iT<sub>reg</sub>)<sup>34</sup>. These iT<sub>reg</sub> expressed Foxp3 mRNA and protein, and showed T cell suppressive function (data not shown). Similar to natural T<sub>reg</sub>, SATB1 was not induced in iT<sub>reg</sub> under these conditions while significantly enhanced expression was observed in cells stimulated via TCR and

CD28 (**Fig. 1f,g**). Moreover,  $T_{H1}$  and  $T_{H2}$  cytokine production was significantly abrogated in the absence of SATB1 (**Fig. 1h**). To determine whether Foxp3 induction in  $iT_{reg}$  was necessary to suppress *SATB1* we performed gain-of-function experiments ectopically over-expressing Foxp3 in  $T_{conv}$  cells. High expression of Foxp3 resulted in reduced expression of SATB1 (**Fig. 1i**), which was accompanied by a concomitant decrease in cytokine expression (**Fig. 1j**) and the induction of a  $T_{reg}$  cell gene signature (**Supplementary Fig. 2**). Less abundant Foxp3 expression did not result in significant repression of *SATB1* or induction of a  $T_{reg}$  cell gene signature (data not shown). Taken together, reduced expression of SATB1 is a hallmark of both  $iT_{reg}$  and  $T_{reg}$  in humans and repression of SATB1 depends on sufficiently high expression of Foxp3.

#### Loss of Foxp3 in $T_{reg}$ results in high SATB1 expression

To further assess the role of Foxp3 in SATB1 repression in human  $T_{reg}$  we performed loss-of-function experiments. Silencing Foxp3 by siRNA resulted in loss of Foxp3 expression as well as genes associated with  $T_{reg}$  cells (**Supplementary Fig. 3**) and consequently loss of suppressive function in  $T_{reg}$  (**Fig. 2a,b**). A small but significant increase of SATB1 expression was evident in unstimulated Foxp3-depleted human  $T_{reg}$  (**Fig. 2c**), however, this was significantly enhanced when  $T_{reg}$  were stimulated via TCR together with co-stimulation or IL-2. This increase in SATB1 expression was associated with production of  $T_{H1}$  (interferon- $\gamma$ , IFN- $\gamma$ ) and  $T_{H2}$  (IL-4 and IL-5) cytokines (**Fig. 2d,e**). As this effect could have been a direct effect of Foxp3 on the cytokine genes themselves we developed a strategy to knockdown SATB1 and Foxp3 simultaneously in human  $T_{reg}$  cells.

Additional knockdown of SATB1 in human  $T_{reg}$  with a silenced *FOXP3* gene (**Supplementary Fig. 4**) resulted in a significantly decreased induction of T helper cytokines (**Fig. 2f**) demonstrating that expression of  $T_{eff}$  cytokines in Foxp3-deficient  $T_{reg}$  cells is governed by SATB1. Similar results were obtained when expanded human  $T_{reg}$  cells were transduced with lentiviruses encoding miR RNAi targeting Foxp3 and SATB1 (**Supplementary Fig. 5**). Together, these findings establish that Foxp3 negatively regulates SATB1 expression and that reducing SATB1 expression is required to prevent expression of  $T_{eff}$  cytokines in human  $T_{reg}$  cells, thus assigning a key function of Foxp3-SATB1 interaction to the  $T_{reg}$  phenotype.

#### Foxp3 is not suppressed by SATB1 in $T_{conv}$ cells

To exclude the possibility that SATB1 may reciprocally repress *FOXP3* in  $T_{conv}$  cells we performed siRNA-mediated knockdown of SATB1 in human naïve  $T_{conv}$  cells to assess whether SATB1 down-regulation in  $T_{conv}$  cells might allow for elevated Foxp3 expression and a conversion of  $T_{conv}$  into  $T_{reg}$  cells (**Supplementary Fig. 6a**). We did not observe increased Foxp3 expression in resting and stimulated naïve  $T_{conv}$  after silencing of SATB1, including  $iT_{reg}$ -inducing conditions (**Supplementary Fig. 6b**). These results suggest that higher SATB1 abundance is not necessary for low expression of Foxp3 in resting  $T_{conv}$  cells and that Foxp3 induction in naïve  $T_{conv}$  cells following stimulation occurs independently of SATB1. In line with this finding, we did not observe increased induction of several  $T_{reg}$  cell associated genes after knockdown of SATB1 (**Supplementary Fig. 6c**).

#### SATB1 expression in mouse $T_{reg}$ cells

To address whether *SATB1* regulation is conserved between human and murine T<sub>reg</sub> we analyzed SATB1 expression by qPCR, immunoblotting, flow cytometry and confocal microscopy in T cells derived from two different Foxp3 reporter mice (DEREG<sup>35</sup>, Foxp3-GFP-Cre<sup>21</sup>). Similar to human T<sub>reg</sub> cells, SATB1 mRNA and protein expression was lower in mouse T<sub>reg</sub> compared with T<sub>conv</sub> cells isolated from thymus, spleen or lymph nodes (**Fig. 3a–c**, and data not shown). SATB1 expression in CD4<sup>+</sup> single-positive thymocytes was considerably higher than in peripheral CD4<sup>+</sup> T<sub>conv</sub> cells from the spleen or lymph nodes (data not shown), which further supports the essential role of SATB1 during early thymocyte development as established in complete *Satb1*<sup>-/-</sup> mice<sup>25</sup>. Despite this, thymic Foxp3<sup>+</sup> T<sub>reg</sub> still displayed a significant down-regulation of SATB1 compared with Foxp3<sup>-</sup> cells.

To establish *Satb1* as a Foxp3 target gene we analyzed T<sub>reg</sub> from male DEREG mice harboring a spontaneously mutated *Foxp3* allele (DEREG x scurfy). Flow-sorted T<sub>reg</sub> from these animals displayed a significantly increased SATB1 expression in T<sub>reg</sub> compared to Foxp3-competent T<sub>reg</sub> (**Fig. 3d**). In line with this finding an increase of T<sub>H1</sub> and T<sub>H2</sub> cytokines *in vivo* was observed in T<sub>reg</sub> from DEREG x scurfy mice (**Fig. 3e**). SATB1 mRNA expression in T<sub>reg</sub> versus T<sub>conv</sub> cells was further validated by reassessment of three transcriptome data sets (GSE18387, GSE6681, GSE11775)<sup>5,36,37</sup> derived from mice with a mutated *Foxp3* gene in T<sub>reg</sub> (data not shown).

Female heterozygous DEREG x scurfy mice harbor both Foxp3-competent and Foxp3-incompetent T<sub>reg</sub> cells. Side-by-side comparison of Foxp3-competent and Foxp3-incompetent T<sub>reg</sub> cells by immunofluorescence revealed a cell-intrinsic function of Foxp3 in repressing SATB1 (**Fig. 3f**). Similar to previous reports we observed nuclear localization of

SATB1 in Foxp3<sup>-</sup> thymocytes forming a cage-like structure within the nucleus (**Fig. 3c**)<sup>26</sup>. Increased SATB1 signals in Foxp3-incompetent T<sub>reg</sub> cells with unchanged localization and distribution further support that SATB1 expression is regulated by Foxp3 (**Fig. 3f**). Upregulation of SATB1 in Foxp3<sup>sf</sup> GFP<sup>+</sup> T<sub>reg</sub> was further quantified by intracellular flow cytometry (**Fig. 3g**). Overall, these data clearly establish increased SATB1 mRNA and protein expression as a consequence of Foxp3 deficiency in T<sub>reg</sub>.

### Foxp3 binds to the *SATB1* locus in human T<sub>reg</sub> cells

Inverse correlation between Foxp3 and SATB1 expression in murine and human T<sub>reg</sub> strongly suggested that Foxp3 might act directly as a transcriptional repressor of the *SATB1* locus. We performed Foxp3-ChIP tiling arrays and promoter arrays using chromatin isolated from human natural T<sub>reg</sub> cells (**Fig. 4a** and **Supplementary Fig. 7a**) as well as bioinformatic *in silico* prediction to identify 16 regions for qPCR validation. Binding regions identified were located upstream of the transcriptional start site as well as in the genomic locus of *SATB1* (**Fig. 4b** and **Supplementary Table 2**). Foxp3 binding within the promoter region or genomic locus of *SATB1* in T<sub>reg</sub> was demonstrated by ChIP-coupled quantitative PCR (ChIP-qPCR) (**Fig. 4c**) and electrophoretic mobility-shift assays (data not shown) clearly demonstrating binding to the *SATB1* locus similar to known targets of Foxp3 (**Supplementary Fig. 7b-f**). To probe functional consequences of Foxp3 binding to the *SATB1* locus, we performed luciferase reporter assays for six of the Foxp3 binding regions. Foxp3 binding regions were cloned in between a minP promoter element and a luciferase reporter gene<sup>38</sup>. Co-transfection of these reporter-constructs with a human *FOXP3* expression vector led to a significant decrease in activity for four of these regions

with more than one Foxp3 binding motif (**Fig. 4d**). Mutation of predicted Foxp3 binding motifs within these regions rescued luciferase activity (**Fig. 4d**) indicating that SATB1 expression is actively repressed by Foxp3 binding to several regions within the genomic *SATB1* locus. Further support for Foxp3 binding was derived from *in vitro* DNA-protein interaction analysis using recombinant Foxp3 protein with either wild-type or mutated Foxp3 binding motifs within the FOXP3-binding regions BR9 and BR10 demonstrating strong binding of Foxp3 only to the wild-type sequences whereas the mutated motifs showed almost no interaction with Foxp3 (**Fig. 4e**). Taken together, these data establish Foxp3 as an important repressor directly binding to the *SATB1* locus in T<sub>reg</sub> cells and preventing SATB1 transcription. .

#### Ectopic SATB1 reprograms human T<sub>reg</sub> to T<sub>eff</sub> *in vitro*

To determine whether reduced SATB1 expression is required for T<sub>reg</sub> to exert regulatory function we overexpressed SATB1 in human natural CD4<sup>+</sup>CD25<sup>hi</sup> Foxp3<sup>+</sup> T<sub>reg</sub> cells using a lentiviral vector carrying the *SATB1* full-length transcript (**Supplementary Fig. 8**). Human T<sub>reg</sub> or T<sub>conv</sub> were stimulated for 24 h with CD3 and CD28-coated beads in the presence of IL-2. After stimulation, T<sub>reg</sub> cells were lentivirally transduced with pELNS DsRED 2A SATB1 which expresses DsRED at a ratio of 1:1 to the transgene<sup>39</sup> or control virus containing only DsRED. Cells were expanded prior to sorting DsRED-positive cells. Only SATB1- and control-transduced cells showing highly similar Foxp3 and DsRED expression were used for further analysis (**Supplementary Fig. 8a**). In sharp contrast to control-transduced T<sub>reg</sub>, SATB1 over-expressing Foxp3<sup>+</sup> T<sub>reg</sub> cells lost their suppressive function (**Supplementary Fig. 8b,c** and **Fig. 5a**). At the same time, these cells gained

expression of  $T_H1$  (IFN- $\gamma$ ),  $T_H2$  (IL-4) and  $T_H17$  (IL-17A) cytokines (**Fig. 5b-e**) suggesting a reprogramming of  $T_{reg}$  cells into  $T_{eff}$  in the presence of abundant SATB1 despite similar Foxp3 expression. As expected,  $T_{conv}$  cells transduced with SATB1 using the same approach had no suppressive function (**Supplementary Fig. 9**). These data strongly support that ectopic expression of SATB1 in  $T_{reg}$  is sufficient to convert the Foxp3-mediated program into  $T_{eff}$  programs.

### High SATB1 expression induces transcriptional $T_{eff}$ programs

To estimate the genome-wide reprogramming in SATB1 over-expressing  $T_{reg}$  cells whole transcriptome analysis was performed. Using stringent filter criteria a total of 100 genes were found to be significantly increased in SATB1-expressing  $T_{reg}$  cells whereas 21 were decreased (**Fig. 6a**). Analysis of the differentially expressed genes revealed that 20% were associated with elevated expression in  $T_{conv}$  (in comparison to  $T_{reg}$ ), 29% of the changed genes were primarily linked with T cell activation, and 16% were classified as common T cell genes. The remaining genes (35%) showed no known association with T cell function or lineage and were classified as SATB1-induced (**Fig. 6b**). Furthermore, compiling gene lists previously associated with  $T_H1$ ,  $T_H2$  and  $T_H17$  differentiation revealed induction of many genes involved in  $T_{eff}$  differentiation in SATB1-expressing  $T_{reg}$  cells (**Fig. 6c**). In contrast genes representing the human  $T_{reg}$  cell gene signature were unchanged in SATB1-expressing  $T_{reg}$  cells (**Fig. 6d**). Since we used polyclonal human  $T_{reg}$  cells for this analysis, it is not surprising that we find the three major T cell differentiation programs simultaneously. In summary, low SATB1 expression in  $T_{reg}$  is necessary to permit

suppressible function and to ensure inhibition of effector cell differentiation of regulatory T cells.

### Epigenetic regulation of *SATB1* transcription in T<sub>reg</sub> cells

The strong dependency of T<sub>reg</sub> function on the repression of *SATB1* implies the involvement of additional regulatory mechanisms. When assessing DNA methylation, we identified three CpG-rich sites upstream of exon 1 at the *SATB1* locus (**Supplementary Fig. 10**). However, in contrast to the *FOXP3* locus itself (**Supplementary Fig. 10a**)<sup>22</sup>, the *SATB1* locus was similarly demethylated in T<sub>reg</sub> and T<sub>conv</sub> cells (**Supplementary Fig. 10b**), suggesting that DNA-methylation does not play a regulatory role at the *SATB1* locus in T<sub>reg</sub> cells.

Next, we examined the chromatin status of the *SATB1* locus by analyzing permissive and repressive histone modifications. ChIP-qPCR of expanded human T<sub>reg</sub> showed a reduction in permissive histone H3 trimethylation at Lys 4 (H3K4me3, **Supplementary Fig. 11a**) and increased repressive histone H3 trimethylation at Lys27 (H3K27me3, **Supplementary Fig. 11b**) in human T<sub>reg</sub> cells compared to T<sub>conv</sub> cells as well as lower acetylation of histone H4 (H4Ac, **Supplementary Fig. 11c**). When assessing a publicly available dataset for murine T<sub>reg</sub> cells<sup>40</sup> we could establish similar histone marks at the *Satb1* locus (**Supplementary Fig. 12**), suggesting that a conserved regulatory circuit exists that contributes to the lower expression of SATB1 in T<sub>reg</sub> by inducing repressive epigenetic marks at the *SATB1* locus.

### MicroRNAs regulate SATB1 in T<sub>reg</sub> cells

A prominent layer of post-transcriptional gene regulation is exerted by miRNAs. MiRNA profiling in human  $T_{\text{reg}}$  versus  $T_{\text{conv}}$  cells allowed us to identify several differentially expressed miRNAs in  $T_{\text{reg}}$  cells (data not shown). Using inverse correlation analysis between SATB1 and miRNA expression as well as computational prediction of miRNA binding of seed-matched sites (**Fig. 7a**), we identified 5 miRNAs that were differentially expressed between  $T_{\text{reg}}$  and  $T_{\text{conv}}$  cells (**Fig. 7b**) and showed a significant inverse correlation between SATB1 and miRNA expression (**Fig. 7c**). Of these 5 miRNAs, miR-155, miR-21, and miR-7 are direct targets of Foxp3 as previously reported for miR-155 (refs. 31,41,42) and miR-21 (ref. 43) and confirmed by Foxp3-ChIP tiling arrays and ChIP-qPCR (**Fig. 7d,e** and **Supplementary Fig. 13**) as well as functional analysis (S. Barry, unpublished data). Assessment of miRNA expression in Foxp3-overexpressing  $T_{\text{conv}}$  cells and Foxp3-silenced  $T_{\text{reg}}$  cells confirmed these miRNAs as targets of Foxp3 (**Supplementary Fig. 14**). For the assessment of functionally relevant binding of the miRNAs to the 3' UTR of the SATB1 mRNA we fused the *SATB1* 3' UTR to a luciferase reporter gene and determined luciferase activity in cells transfected with synthetic miRNAs. Expression of any of the 5 miRNAs significantly repressed constitutive luciferase activity with the 3 miRNAs that are direct targets of Foxp3 clearly showing the strongest effect (**Fig. 7f**). Mutation of the respective binding motifs resulted in restoration of luciferase activity (**Fig. 7f**). As exemplified for miR-155, loss of function of a single miRNA only resulted in minor differences in SATB1 mRNA expression in primary human  $T_{\text{reg}}$  (**Supplementary Fig. 15a**) indicating that the loss of a single miRNA may be incapable of rescuing SATB1 expression. Complete loss of all miRNAs, however, as achieved in mice

by a  $T_{\text{reg}}$ -specific deletion of *Dicer1* (ref. 21) clearly lead to up-regulation of SATB1 at both mRNA and protein level (**Fig. 7g** and **Supplementary Fig. 15b**). These results suggest that Foxp3 is able to confer  $T_{\text{reg}}$ -specific down-regulation of SATB1 expression not only by direct binding to the *Satb1* locus but also using a second layer of regulation using miRNAs.

#### Abundant SATB1 expression decreases $T_{\text{reg}}$ function *in vivo*

To assess whether SATB1 expression results in reduced regulatory function in mouse  $T_{\text{reg}}$  *in vitro* and *in vivo* we overexpressed SATB1 in mouse  $CD4^+$   $Foxp3^+$   $T_{\text{reg}}$  cells from DEREK mice using a lentivirus encoding the *Satb1* full-length transcript (**Supplementary Fig. 16**). Sorted  $CD4^+$   $Foxp3^+$   $T_{\text{reg}}$  cells from DEREK mice were expanded for 10-14 days with CD3 and CD28-coated beads in the presence of IL-2. After this initial expansion period, expanded  $T_{\text{reg}}$  cells were transduced with a SATB1-IRES-Thy1.1 or control lentivirus. Cells were expanded for 4 additional days in the presence of CD3 and CD28-coated beads and IL-2 prior to sorting Thy1.1-positive  $GFP^+$   $T_{\text{reg}}$ . SATB1 and control-transduced  $T_{\text{reg}}$  had similar Foxp3 expression (**Supplementary Fig. 16a**). In contrast to control-transduced  $T_{\text{reg}}$  cells, the overexpression of SATB1 in  $Foxp3^+$   $T_{\text{reg}}$  cells resulted in a loss of suppressive function and acquisition of  $T_{\text{H1}}$  (IFN- $\gamma$ ) and  $T_{\text{H2}}$  (IL-5) effector cytokine expression (**Fig. 8a,b** and **Supplementary Fig. 16b-f**) supporting a reprogramming of  $T_{\text{reg}}$  cells into  $T_{\text{eff}}$  cells in the presence of significantly elevated SATB1 expression.

To assess *in vivo* suppressor capacity of the manipulated T<sub>reg</sub> cells, control T<sub>reg</sub> or T<sub>reg</sub> cells overexpressing SATB1 were transferred together with naïve CD4<sup>+</sup>CD45RB<sup>hi</sup> T cells (isolated from normal mice) into *Rag2*<sup>-/-</sup> recipient mice. Transfer of naïve CD4<sup>+</sup>CD45RB<sup>hi</sup> T cells alone led to the development of colitis (**Fig. 8c-e**). As expected, *Rag2*<sup>-/-</sup> mice that received naïve CD4<sup>+</sup>CD45RB<sup>hi</sup> T cells and control-transduced T<sub>reg</sub> cells did not show colitis-associated pathology (**Fig. 8c-e**) while mice receiving only naïve CD4<sup>+</sup>CD45RB<sup>hi</sup> cells had colonic infiltrates and weight loss. Transfer of SATB1-overexpressing T<sub>reg</sub> cells together with naïve CD4<sup>+</sup>CD45RB<sup>hi</sup> T cells resulted in colitis-associated pathology suggesting an impairment in suppressor function of SATB1-overexpressing T<sub>reg</sub> cells concomitant with a gain of effector function (**Fig. 8c-e**). We observed a significant expansion in the number of T<sub>conv</sub> cells in mice receiving either no T<sub>reg</sub> cells or SATB1-overexpressing T<sub>reg</sub> cells in spleen, mesenteric and peripheral lymph nodes (**Fig. 8f**), while the number of cells that maintained Foxp3 expression in spleen, mesenteric and peripheral lymph nodes was equal in mice receiving control vector-transduced or SATB1-overexpressing T<sub>reg</sub> cells (**Fig. 8g**). Thus, Foxp3<sup>+</sup> T<sub>reg</sub> cells expressing elevated amounts of SATB1 show lower suppressor function with a concomitant gain of T<sub>eff</sub> programs *in vivo* and *in vitro* suggesting that down-regulation of SATB1 in T<sub>reg</sub> cells is necessary to maintain a stable suppressive phenotype (**Supplementary Fig. 17**).

## DISCUSSION

In  $T_{\text{reg}}$  numerous mechanisms have been implicated in their suppressive function upon contact to other immune effector cells<sup>1</sup>. At the same time intrinsic inhibition of  $T_{\text{eff}}$  function mainly by FOXP3-induced mechanisms seems to be necessary for  $T_{\text{reg}}$  to exert suppressive function. In this report we identified the repression of SATB1 in  $T_{\text{reg}}$  to be required for suppressive function and inhibition of effector differentiation of these cells. As up-regulation of SATB1 is required for the induction of  $T_{\text{eff}}$  cytokines in  $T_{\text{conv}}$  the profound lack of up-regulation of SATB1 following stimulation in  $T_{\text{reg}}$  suggests that FOXP3-mediated suppression of SATB1 plays an important role in inhibiting cytokine production within a  $T_{\text{reg}}$ . In support of this, ectopic expression of high levels of SATB1 in  $T_{\text{reg}}$  led to the induction of  $T_{\text{eff}}$  cytokines and loss of suppressive function despite the expression of FOXP3 *in vitro* and *in vivo*. Mechanistically, SATB1 expression is controlled directly by FOXP3-mediated transcriptional repression, histone modifications as well as the induction of miRNAs binding to the 3'UTR of SATB1. Together these findings establish that continuous active repression of central mechanisms involved in  $T_{\text{eff}}$  programs provided by SATB1 is necessary for  $T_{\text{reg}}$  to exert their suppressive function.

Thus a major finding of our study is that  $T_{\text{reg}}$  not only depend on the induction of FOXP3-mediated genes associated with suppressive function but also on the specific repression of molecules such as SATB1 to prevent  $T_{\text{eff}}$  function. SATB1 expression at low levels seems to be necessary to retain functional T-cell integrity not only in  $T_{\text{conv}}$  but also in  $T_{\text{reg}}$  as complete SATB1 KO are basically devoid of T cells in the periphery<sup>25</sup>. While FOXP3 clearly dictates the repression of SATB1 in  $T_{\text{reg}}$  thereby preventing  $T_{\text{eff}}$  function, we have no evidence so far for an inverse control of FOXP3 by SATB1 in  $T_{\text{conv}}$ , which

together favors a model with  $T_{\text{eff}}$  programs continually and actively overruled by FOXP3-mediated transcriptional repression within a  $T_{\text{reg}}$ .

Further evidence for such a model comes from studies elucidating the effect of the transcriptional repressor Eos in  $T_{\text{reg}}$ <sup>13</sup>. Eos directly interacts with FOXP3 to specifically induce chromatin modifications that result in gene silencing, while genes induced by FOXP3 were not affected. Interestingly, loss of Eos abrogated suppressive  $T_{\text{reg}}$  function but only partially endowed  $T_{\text{reg}}$  with  $T_{\text{eff}}$  functions consistent with the normal repression of  $T_{\text{eff}}$  differentiation within a  $T_{\text{reg}}$ . Similarly, loss of Runx1-CBF $\beta$  heterodimers, another component of the FOXP3 containing multi-protein complex, in  $T_{\text{reg}}$  leads to reduction of FOXP3 expression, loss of suppressor function and gain of IL-4 expression by  $T_{\text{reg}}$ <sup>44,45</sup>. FOXP3 as well as Eos and Runx1-CBF $\beta$  heterodimers have been shown to directly repress certain effector cytokines such as IFN- $\gamma$  or IL-4 suggesting  $T_{\text{reg}}$  may use multiple mechanisms to suppress  $T_{\text{eff}}$  programs<sup>13,18,44</sup>. Nevertheless, the ectopic expression of SATB1 in  $T_{\text{reg}}$  was sufficient to induce effector cytokines suggesting that high levels of SATB1 can overcome FOXP3 repression of downstream targets. This might be similarly true in activated  $T_{\text{conv}}$  that can express lower levels of FOXP3 temporarily during early activation phases.

Recently the FOXO transcription factors Foxo1 and Foxo3 have also been implicated in the inhibition of  $T_{\text{eff}}$  function in  $T_{\text{reg}}$ <sup>14</sup>. Interestingly, lack of Foxo1 and Foxo3 in  $T_{\text{reg}}$  is sufficient to induce TH1 and TH17 effector cytokines but not TH2 cytokines whereas SATB1 seems to have a more profound effect on TH2 cytokines under certain conditions<sup>29,46</sup>. Together these findings point to a hierarchy of repressive mechanisms ensuring suppression of  $T_{\text{eff}}$  function in  $T_{\text{reg}}$ .

Our findings support a model of continuously active regulatory networks shaping the overall function of T cells in the periphery as an alternative to terminal differentiation. An active and continuous blockade of  $T_{\text{eff}}$  function instead of terminal  $T_{\text{reg}}$  differentiation allows T cells a higher degree of functional plasticity e.g. under inflammatory conditions where  $T_{\text{reg}}$  can gain effector function once FOXP3 is switched off<sup>24,47-49</sup>.

## METHODS

Methods and any associated references are available in the online version of the paper at <http://www.nature.com/natureimmunology/>.

**Accession codes.** GEO: microarray data, GSE15390; tiling array data, GSE20995.

Note: Supplementary information is available on the Nature Immunology website.

## ACKNOWLEDGMENTS

We thank M. Mai, M. Kraut, S. Keller, N. Kuhn, J. Birke, I. Büchmann, A. Dolf, and P. Wurst for technical assistance, M. Hoch, M. Pankratz, S. Burgdorf, A. Popov, A. Staratschek-Jox as well as all other lab members for discussions and J. Oldenburg for providing us with blood samples from healthy individuals. J.L.S. and M.B. are funded by the German Research Foundation (SFB 832, SFB 704, INST 217/576-1, INST 217/577-1), the Wilhelm-Sander-Foundation, the German Cancer Aid, the German Jose-Carreras-Foundation, the BMBF (NGFN2), and the Humboldt-Foundation (Sofja-Kovalevskaja Award). B.R.B. and K.L.H. are funded by a translational research grant from the Leukemia and Lymphoma Society of America (R6029-07). X.Z., S.L.B.-B., and J.A.B. are funded by the Juvenile Diabetes Research foundation Scholar #16-2008-643, and UCSF Autoimmunity Center of Excellence. S.C.B. supported by NHMRC project grants 339123, 565314. B.S. is funded by the German Research Foundation (SCHE 1562; SFB832). S.B. T.G. and J.L.R. are funded by JDRF Collaborative Centers for Cell Therapy and the JDRF Center on Cord Blood Therapies for Type 1 Diabetes.

## AUTHOR CONTRIBUTIONS

M.B. designed, performed and supervised experiments, analyzed data, wrote the manuscript; Y.T. performed qPCR, CBA, WB, overexpression experiments and filter retention analysis, analyzed data; R.M. designed and performed reporter assays; S.C. performed experiments, analyzed data; T.S. performed CHIP experiments, analyzed data; K.L. and C.T.M. performed experiments with DEREK mice; S.B. and T.G. performed overexpression experiments; E.S. performed and analyzed immunofluorescence experiments; W.K. performed histone methylation studies, S.L.B.-B. and X.Z. performed experiments with *Dicer1<sup>fl/fl</sup>* mice; A.H. performed bioinformatic analysis; D.S. generated lentiviral constructs; S.D.P. performed microarray experiments; E.E. performed FACS sorting; J.B. and A.L. performed experiments with *Rag2<sup>-/-</sup>* mice; P.A.K. was involved in study design; K.L.H. and B.R.B. provided vital analytical tools; R.B. provided vital analytical tools; T.Q. supervised and analyzed immunofluorescence experiments; C.W. performed IHC; A.W. performed, designed and supervised DNA methylation experiments; G.M. and M.F. designed and supervised filter retention experiments; W.K. designed and supervised experiments, wrote the manuscript; B.S. designed and analyzed reporter assays; S.C.B. designed and supervised CHIP experiments; T.S. designed and supervised experiments with DEREK mice, provided vital analytical tools; J.A.B. designed and supervised experiments with *Dicer1<sup>fl/fl</sup>* mice; J.L.R. designed and supervised SATB1 overexpression experiments, wrote the manuscript; J.L.S. designed, supervised and analyzed experiments, wrote the manuscript. All authors discussed the results and commented on the manuscript.

## COMPETING FINANCIAL INTERESTS

Research support to J.L.S. and M.B. has in part been provided by Becton Dickinson.

R.B. is currently employed by Becton Dickinson, S.C. by Miltenyi Biotech.

J.L.S., M.B. and R.B. have applied for several US and international patents on T<sub>reg</sub> cell biology.

Published online at <http://www.nature.com/natureimmunology/>.

Reprints and permissions information is available at <http://npg.nature.com/reprintsandpermissions/>.

## Figure Legends

**Figure 1.** Foxp3-dependent repression of SATB1 expression in human T<sub>reg</sub> cells.

(a) Microarray analysis of SATB1 mRNA expression in human T<sub>conv</sub> and T<sub>reg</sub> (Rest=resting, Act=activated, TGF=TGF- $\beta$  treated, Exp=expanded). (b) Relative SATB1 mRNA expression in human T<sub>reg</sub> and T<sub>conv</sub>. (c) Immunoblotting (left) for SATB1 (top) and  $\beta$ -actin (bottom) in human T<sub>reg</sub> and T<sub>conv</sub>, and densitometric analysis to quantify ratio of SATB1 to  $\beta$ -actin (right). (d) SATB1 expression was determined by flow cytometry (left) in human T<sub>reg</sub> and T<sub>conv</sub> with quantification shown in the graph at right. (e) SATB1 expression was determined by flow cytometry after stimulation of human T<sub>reg</sub> and T<sub>conv</sub> for 2 d (left) with quantification shown normalized to resting T<sub>conv</sub> in the graph at right. (f) Relative SATB1 mRNA expression in human iT<sub>reg</sub>, stimulated T cells (stim T) and unstimulated T cells (unstim T) on day 5. (g) SATB1 expression was determined by flow cytometry in human iT<sub>reg</sub>, stim T and unstim T (left) with quantification shown in the graph at right. (h) Cytometric bead assay for IL-4 and IFN- $\gamma$  secretion in the supernatants of human iT<sub>reg</sub>, stim T and unstim T. (i) Relative Foxp3 (left) and SATB1 mRNA expression (right) in T<sub>conv</sub> lentivirally transduced with Foxp3 vector (Foxp3 vector) or control vector (Ctrl vector) rested for 3 days. (j) Relative IL-5 (left) and IFN- $\gamma$  mRNA expression (right), assessed and presented as in i. \*P < 0.05 (Student's *t*-test). Numbers in plots indicate mean fluorescence intensity (d,e). Data are representative of five experiments (b,e,i,j; mean and s.d.), six experiments (c,f; mean and s.d.), three experiments (g; mean and s.d.), eleven experiments (d;

mean and s.d.), or three independent experiments (**h**; mean  $\pm$  s.d. of triplicate wells), each with cells derived from a different donor.

**Figure 2.** Rescue of SATB1 expression after silencing of Foxp3 in T<sub>reg</sub> cells.

(a) Foxp3 expression was determined by flow cytometry (left) in human T<sub>reg</sub> transfected with siRNA targeting Foxp3 (Foxp3 siRNA) or nontargeting (control) siRNA (Ctrl siRNA) 48 h post knockdown with quantification shown in the graph at right. \*P < 0.05 (Student's *t*-test). (b) Suppression of allogeneic CD4<sup>+</sup> T cells, labeled with the cytosolic dye CFSE (responding T cells (T<sub>resp</sub>)) by human T<sub>reg</sub> transfected with siRNA targeting Foxp3 (Foxp3 siRNA) or nontargeting (control) siRNA (Ctrl siRNA), presented as CFSE dilution in responding T cells cultured with CD3+CD28-coated beads and T<sub>reg</sub> at a ratio of 1:1 or without T<sub>reg</sub> (T<sub>resp</sub> only). (c) Relative SATB1 mRNA expression in human T<sub>reg</sub> after silencing of Foxp3. T<sub>reg</sub> were transfected and cultivated for 48 hours without stimulation (Rest) or in the presence of CD3 and IL-2 ( $\alpha$ -CD3+IL-2) or CD3 and CD28 ( $\alpha$ -CD3+ $\alpha$ -CD-28). \*P < 0.05 (Student's *t*-test). (d) Relative IL-5 (left) and IFN- $\gamma$  mRNA expression (right) in siRNA-treated T<sub>reg</sub> stimulated for 48 hours in the presence CD3 and IL-2. \*P < 0.05 (Student's *t*-test). (e) Cytometric bead assay for IL-4 and IFN- $\gamma$  secretion in the supernatants of siRNA-treated T<sub>reg</sub> stimulated as in d. \*P < 0.05 (Student's *t*-test). (f) Relative IL-5 (left) and IFN- $\gamma$  mRNA expression (right) in T<sub>reg</sub> transfected with nontargeting (control) siRNA (Ctrl siRNA), Foxp3-targeting siRNA (Foxp3 siRNA) or Foxp3- and SATB1-targeting siRNA (Foxp3 + SATB1 siRNA) followed by stimulation with CD3+CD28-coated beads for 48 hours. \*P < 0.05 (one-way ANOVA with LSD). Data are representative of six experiments (a,c; mean and s.d.), four experiments (d,f; mean and s.d.), three independent experiments (b), or three independent experiments (e; mean  $\pm$  s.d. of triplicate wells), each with cells derived from a different donor.

**Figure 3.** Foxp3-dependent repression of SATB1 expression in mouse T<sub>reg</sub> cells.

(a) SATB1 expression was determined by flow cytometry (left) in freshly isolated T<sub>reg</sub> and T<sub>conv</sub> from spleen of male DEREK mice with quantification shown in the graph at right. \*P < 0.05 (Student's *t*-test). (b) Immunoblotting for SATB1 (top) and Erk1, Erk2 (bottom) in mouse T<sub>reg</sub> and T<sub>conv</sub>. (c) Z-projection of immunofluorescence for SATB1 (red) and GFP (green) in thymocytes from male DEREK mice; nuclei are stained with the DNA-intercalating dye DAPI. White arrow depicts T<sub>reg</sub>. (d) Relative SATB1 mRNA expression in CD4<sup>+</sup>GFP<sup>+</sup> (T<sub>reg</sub>) and CD4<sup>+</sup>GFP<sup>-</sup> (T<sub>conv</sub>) T cells from male DEREK or Foxp3-deficient DEREK x scurfy mice. \*P < 0.05 (Student's *t*-test). (e) Relative IL-6 (left) and IFN- $\gamma$  mRNA expression (right) in CD4<sup>+</sup>GFP<sup>+</sup> T<sub>reg</sub> derived from male DEREK or Foxp3-deficient DEREK x scurfy mice. \*P < 0.05 (Student's *t*-test). (f) Confocal microscopy for SATB1 (red) and Foxp3 (green) in thymic T<sub>reg</sub> from female DEREK mice heterozygous for the scurfy mutation counterstained with DAPI (blue). CD4<sup>+</sup>GFP<sup>+</sup>FOXP3<sup>-</sup> Foxp3-deficient T<sub>reg</sub> (top, Foxp3<sup>sf</sup>) or CD4<sup>+</sup>GFP<sup>+</sup>FOXP3<sup>+</sup> Foxp3-competent T<sub>reg</sub> (bottom, Foxp3<sup>wt</sup>). (g) SATB1 expression was determined by flow cytometry (left) in thymic single positive CD4<sup>+</sup>GFP<sup>+</sup>FOXP3<sup>+</sup> (left, grey) and CD4<sup>+</sup>GFP<sup>+</sup>FOXP3<sup>-</sup> T<sub>reg</sub> (right, black) from female DEREK mice heterozygous for the scurfy mutation with quantification shown in the graph at right. Isotype control shown as solid line. Numbers in plots indicate mean fluorescence intensity (a,g). Data are representative of three independent experiments (a; mean and s.d.), two independent experiments (g; mean and s.d.), two independent experiments (c,f,b), or two independent experiments (d,e; mean  $\pm$  s.d. of triplicate wells).

**Figure 4.** Direct suppression of *SATB1* transcription by Foxp3.

(a) Foxp3 ChIP tiling array data (blue) from human expanded cord-blood  $T_{reg}$ . Data were analyzed with MAT and overlaid to the *SATB1* locus to identify binding regions (1-13,  $p < 10^{-5}$  and FDR < 0.5%). Data are representative of two independent experiments with cells derived from different donors. (b) Schematic representation of Foxp3 binding regions (BR) at the human genomic *SATB1* locus identified by *in silico* prediction within the regions identified in a. (c) ChIP analysis of human expanded cord-blood  $T_{reg}$  cells with a Foxp3-specific antibody and PCR primers specific for Foxp3 binding regions. Relative enrichment of Foxp3 ChIP over input normalized to IgG was calculated. A region -15 kb upstream (-15kb) was used as a negative control. \* $P < 0.05$  (Student's *t*-test). Data are representative of three independent experiments (mean and s.d.) with cells derived from different donors. (d) Luciferase assay of FOXP3 binding to the respective binding regions at the *SATB1* locus in HEK293T cells, transfected with luciferase constructs containing wild-type (WT) or mutated (Mut) binding regions BR9-14 of the *SATB1* locus (with mutation of the Foxp3-binding motifs), together with a FOXP3 encoding expression vector or control vector (Ctrl). \* $P < 0.05$  (Student's *t*-test). Data is from one representative experiment of two (mean and s.d. of triplicate wells). Numbers indicate Foxp3-binding motifs within each region. (e) Determination of the  $K_D$ -values of Foxp3 binding to a wild-type (WT) or mutated (Mut) Foxp3 binding motif in BR9 and BR10 at the *SATB1* locus by filter retention analysis. Data are representative of three independent experiments (mean and s.d. of triplicates).

**Figure 5.** SATB1 expression in human T<sub>reg</sub> reprograms T<sub>reg</sub> into effector T cells.

(a) Suppression of CD8<sup>+</sup> T cells, labeled with the cytosolic dye CFSE (CD8<sup>+</sup> T cells) by human T<sub>reg</sub> lentivirally transduced with SATB1 (T<sub>reg</sub> cells (SATB1), blue) or control vector (T<sub>reg</sub> cells (Ctrl), red), presented as CFSE dilution in responding T cells cultured with CD3-coated beads and T<sub>reg</sub> at a ratio of 1:1 or without T<sub>reg</sub> (CD8<sup>+</sup> T cells only; left), and as percent proliferating CD8<sup>+</sup> T cells versus the T<sub>reg</sub> cell/CD8<sup>+</sup> T cell ratio (right). Data are representative of three independent experiments (mean and s.d.) with cells derived from different donors. (b) Cytometric bead assay for IL-4 and IFN- $\gamma$  secretion in the supernatants of human T<sub>reg</sub> lentivirally transduced with SATB1 (T<sub>reg</sub> cells (SATB1), blue) or control vector (T<sub>reg</sub> cells (Ctrl), red) assessed 4 and 16 h after stimulation with CD3+CD28-coated beads. \*P < 0.05 (Student's *t*-test). Data is from one representative experiment of two (mean and s.d. of triplicate wells) with cells derived from different donors. (c-e) Relative IL-5 (c), IFN- $\gamma$  (d), and IL-17A (e) mRNA expression (right) in human T<sub>conv</sub> (grey) and T<sub>reg</sub> lentivirally transduced with SATB1 (T<sub>reg</sub> cells (SATB1), blue) or control vector (T<sub>reg</sub> cells (Ctrl), red) activated for 16 h with CD3+CD28-coated beads. \*P < 0.05 (Student's *t*-test). Data is from one representative experiment of two (mean and s.d. of triplicate wells) with cells derived from different donors.

**Figure 6.** Transcriptional  $T_{\text{eff}}$  programs are induced in SATB1 expressing  $T_{\text{reg}}$

(a) Microarray analysis of human  $T_{\text{reg}}$  lentivirally transduced with SATB1 (SATB1) or control vector (Ctrl) after 16 hours stimulation with CD3+CD28-coated beads, presented as a heat map of differentially expressed genes. Data were z-score normalized. (b) Cross annotation analysis using 4 classes: genes associated with  $T_{\text{conv}}$  but not  $T_{\text{reg}}$  cells ( $T_{\text{conv}}$  cell-dependent, yellow), with T cell activation (activation-dependent, green), common T-cell genes (common, orange), and SATB1-induced genes (SATB1-induced, black). Numbers indicate genes within each group. (c) Visualization of gene expression levels of genes previously associated with  $T_{\text{H1}}$ ,  $T_{\text{H2}}$ , or  $T_{\text{H17}}$  differentiation, presented as a heat map. Data were z-score normalized. P values for  $T_{\text{H}}$  associated genes determined by  $\chi^2$  test in comparison to the complete data set ( $T_{\text{H}}$  specific gene enrichment):  $T_{\text{H1}}$ ,  $P = 3.24 \times 10^{-6}$ ;  $T_{\text{H2}}$ ,  $P = 9.03 \times 10^{-15}$ ;  $T_{\text{H17}}$ ,  $P = 1.16 \times 10^{-6}$ . (d) Changes in genes associated with the human  $T_{\text{reg}}$  signature as assessed in  $T_{\text{reg}}$  lentivirally transduced with SATB1 (SATB1) in comparison to control vector (Ctrl). The mean  $\log_2$  fold-changes of the comparison  $T_{\text{reg}}$  to  $T_{\text{conv}}$  (red dots) and SATB1 to control-transduced  $T_{\text{reg}}$  (blue dots) were plotted and both comparisons were ranked by fold change in the  $T_{\text{reg}}$  vs.  $T_{\text{conv}}$  comparison. Data are derived from three independent experiments with cells derived from different donors.

**Figure 7.** SATB1 expression is repressed by miRNA in T<sub>reg</sub>.

(a) Representation of the human genomic *SATB1* 3' UTR and the conserved miRNA binding sites. (b) Relative miR-155, miR-21, miR-7, miR-34a, and miR-18a expression human T<sub>reg</sub> and T<sub>conv</sub>. \*P < 0.05 (Student's *t*-test). Data are representative of five experiments (mean and s.d.) with cells derived from different donors. (c) Correlation of miRNA expression with SATB1 mRNA expression is plotted against miRNA fold change (T<sub>reg</sub> vs. T<sub>conv</sub>) for all 735 miRNA assessed by microarrays. Highlighted are miR-155, miR-21, miR-7, miR-34a, and miR-18a. Data are representative of three experiments with cells derived from different donors. (d) Foxp3 ChIP tiling array data (blue) for miR-155, miR-21, and miR-7 from human expanded cord-blood T<sub>reg</sub>. Data were analyzed with MAT and overlaid to the respective locus to identify binding regions (P < 10<sup>-5</sup> and FDR < 0.5%). Data are representative of two independent experiments with cells derived from different donors. (e) ChIP analysis of human expanded cord-blood T<sub>reg</sub> cells with a Foxp3-specific antibody and PCR primers specific for miR-155, miR-21, and miR-7. Relative enrichment of Foxp3 ChIP over input normalized to IgG was calculated. The AFM locus was used as a negative control. \*P < 0.05 (Student's *t*-test). Data are representative of three independent experiments (mean and s.d.) with cells derived from different donors. (f) Dual-luciferase assay of HEK-293T cells transfected with luciferase constructs containing wild-type (WT) 3' UTR or mutated (Mut) 3' UTR of *SATB1* (with mutation of the miRNA-responsive elements), together with synthetic mature miRNAs or a synthetic control miRNA (Ctrl). \*P < 0.05 (Student's *t*-test). Data are representative of three independent experiments (mean and s.d.). (g) Immunoblotting for SATB1 (top) and Erk1, Erk2 (bottom) in T<sub>reg</sub> from mice with a T<sub>reg</sub>-specific complete DICER loss (*Dicer1*<sup>fl/fl</sup>) in

comparison to *Dicer1*<sup>+/fl</sup> T<sub>reg</sub>. Data are representative of two independent experiments.

**Figure 8.** Ectopic expression of SATB1 in  $T_{reg}$  results in reduced suppressive function *in vivo*.

(a) Suppression of  $CD4^+$  T cells, labeled with the cytosolic dye eFluor 670 ( $T_{conv}$  cells) cultured with CD3+CD28-coated beads by expanded mouse  $T_{reg}$  lentivirally transduced with SATB1 (SATB1, blue) or control vector (Ctrl, red), presented as percent proliferating  $T_{conv}$  cells versus the  $T_{reg}$  cell/ $T_{conv}$  cell ratio (right). (b) Relative IL-5 (left) and IFN- $\gamma$  mRNA expression (right) in murine  $T_{reg}$  lentivirally transduced with SATB1 (SATB1, blue) or control vector (Ctrl, red). (c) Hematoxylin and eosin staining of colon sections from  $Rag2^{-/-}$  mice at 9 weeks after the transfer of  $CD4^+CD45RB^{hi}$  naive T cells (naïve T) alone or in combination with control-transduced  $T_{reg}$  ( $T_{reg}$  cells (Ctrl)) or SATB1-transduced  $T_{reg}$  ( $T_{reg}$  cells (SATB1)). Original magnification,  $\times 200$ ; scale bars, 100  $\mu m$ . (d) Histology scores of colon sections of  $Rag2^{-/-}$  mice at 9 weeks after the transfer in c. (e) Body weight of  $Rag2^{-/-}$  mice at 9 weeks after the transfer in c, presented relative to initial body weight. (f,g) Recovery of  $T_{conv}$  (f) and  $T_{reg}$  (g) from spleens, mesenteric, and peripheral lymph nodes of  $Rag2^{-/-}$  mice at 9 weeks after the transfer in c. \* $P < 0.05$  (Student's *t*-test). NS, not significant. Data are representative of three independent experiments (b; mean and s.d.), two independent experiments (a; mean and s.e.m. of triplicate cultures), or are pooled from two independent experiments (c-g; mean and s.d. of four resp. five recipient mice).

## ONLINE METHODS

### Mice.

DEREG, scurfy, DEREG x scurfy, Foxp3-GFP-hCre BAC x *Dicer1*<sup>fl/fl</sup>, and Foxp3-GFP-hCre BAC x *Dicer1*<sup>fl/fl</sup> x ROSA26R-YFP mice were previously described<sup>4,21,35,50</sup>.

All animal experiments were approved by the responsible Institutional Animal Care and Use Committee (University of California, San Francisco, Lower Saxony, Germany or North Rhine Westfalia, Germany).

### Antibodies and flow cytometry analysis.

Fluorescent-dye-conjugated antibodies were purchased from Becton Dickinson, BioLegend, or eBioscience. Alexa 647-conjugated mouse anti-human SATB1 monoclonal antibody (clone 14) cross-reactive to mouse SATB1 was prepared by R. Balderas (BD Biosciences). Intracellular staining of human and murine Foxp3 and SATB1 was conducted using either the human or mouse Foxp3 Regulatory T-cell Staining Kit (BioLegend).

### Purification and sorting of human T<sub>reg</sub> cells

Human T<sub>reg</sub> and T<sub>eff</sub> cells were purified from whole blood of healthy human donors in compliance with institutional review board protocols (Ethics committee of the University of Bonn) by negative selection using CD4-RosetteSep (Stem Cell), followed by positive-selection using CD25-specific MACS beads (Miltenyi Biotec) or sorting on a FACSDiVa or Aria III cell sorter (Becton Dickinson) after incubating cells with combinations of fluorochrome-labeled monoclonal antibodies to CD4, CD25, and CD127.

**qRT-PCR.**

Total RNA extracted using TRIZOL (Invitrogen) was used to generate cDNA along with the Transcriptor First Strand cDNA synthesis kit (Roche Diagnostics). qRT-PCR was performed using the LightCycler Taqman master kit and the Universal Probe Library assay on a LightCycler 480 II (Roche Diagnostics). Results were normalized to housekeeping gene expression.

**Immunoblot analysis.**

Cell lysates from purified cells were prepared as previously described<sup>51</sup> followed by immunoblotting with SATB1 antibody (BD, clone 14) as well as human beta-actin (Millipore, C4) or murine Erk1, Erk2 antibody (Cell signaling, L34F12) as loading control.

**Whole-genome gene expression in human cells.**

All RNA was extracted using TRIZOL (Invitrogen) and purified in our laboratory using standard methods. Sample amplification, labeling and hybridization on Illumina WG6 Sentrix BeadChips V1 or V3 were performed for all arrays according to the manufacturer's instructions (Illumina). All data analyses were performed by using Bioconductor for the statistical software R (<http://www.r-project.org>).

**Immunofluorescence microscopy.**

Unpurified lymphocytes from male DERE<sup>G</sup> or CD4<sup>+</sup> GFP<sup>+</sup> T<sub>reg</sub> cells from female heterozygous DERE<sup>G</sup> x scurfy mice purified from thymus were fixed in cold

paraformaldehyde for 10 min, washed with PBS, permeabilized with Triton-X and pre-blocked in PBS containing 10% normal goat serum and 1% gelatine from cold water fish skin for 30 min. Slides were then incubated in combinations of primary antibodies (rabbit anti-GFP (Invitrogen), mouse anti-Foxp3 (eBioscience, eBio7979), mouse anti-SATB1-AF647 (BD Biosciences, clone 14)) for 60 min, washed twice, and incubated with secondary antibodies (anti-rabbit-AF488, anti-mouse-AF555, Invitrogen) for 60 min, stained with DAPI and fluorescence was examined using an Olympus FluoView FV1000 or Zeiss LSM 5 LIVE confocal microscope.

#### **Chromatin immunoprecipitation, whole genome arrays, and ChIP qPCR.**

Expanded human cord blood T<sub>reg</sub> cells were cultured overnight before stimulation with Ionomycin before cross-linking for 10 min in 1% formaldehyde solution. Cell lysis, chromatin immunoprecipitation (ChIP), DNA isolation steps, as well as data acquisition and analysis for human Foxp3 ChIP-on-chip experiments were carried out as previously described<sup>52</sup>.

Validation of Foxp3 binding to genomic regions was carried out by ChIP-qPCR. Reactions were performed using a RT2 SYBRgreen/ROX qPCR master mix (SABiosciences). The relative enrichment of target regions in Foxp3 immunoprecipitated material relative to input chromatin analysis was carried out using the  $2^{-\Delta\Delta CT}$  method. Immunoprecipitations using rabbit IgG were used to normalize for non-specific background.

#### **Gene-specific mRNA silencing, miRNA knockdown and agonistic miRNA.**

All siRNAs as well as the miRNA mimics and inhibitors were purchased from Biomers or Dharmacon. miRNA mimics were designed according to the sequences published in miRBase and resembling the double-stranded Dicer-cleavage products. miRNA-inhibitors were designed as single-stranded antisense 2'OM oligonucleotides. These were used for transfection of freshly isolated primary human T<sub>reg</sub> cells with nucleofection. For luciferase assays, HEK293T cells were transfected with both the reporter plasmids and the small RNA duplexes using Lipofectamine 2000 in a 96-well format and luciferase activity was measured 24 h later.

#### **miRNA profiling and miRNA qRT-PCR.**

All RNA were extracted using TRIZOL (Invitrogen) and purified using standard methods. Sample amplification, labeling and hybridization on Illumina miRNA array matrix were performed with the human v1 MicroRNA Expression Profiling kit for all arrays in this study according to the manufacturer's instructions (Illumina) using an Illumina BeadStation. All data analyses were performed by using Bioconductor for the statistical software R (<http://www.r-project.org>). For miRNA-specific qRT-PCR, total RNA was extracted using TRIZOL. First strand complementary DNA for each miRNA assessed was synthesized by using the TaqMan MicroRNA RT kit and the corresponding miRNA specific kit (Applied Biosystems). Abundance of miRNA was measured by qPCR using the TaqMan Universal PCR MasterMix (Applied Biosystems) on a LighCycler 480 II (Roche Diagnostics). Ubiquitously expressed U6 small nuclear RNA or miR-26b were used for normalization.

**Cloning of *SATB1* 3'UTR constructs.**

The *SATB1* 3'UTR was amplified by PCR using human genomic DNA as source material. The full-length 3'UTR construct was amplified with primers covering the full 1.2 kB region. After digestion with Xho I and NotI the fragment was cloned into the psiCHECK II vector (Promega) to generate psiCHECK II-*SATB1*-3'UTR.

A mutated construct was generated with PCR-based mutagenesis or the QuikChange Lightning Multi Site-Directed mutagenesis kit (Stratagene) following the manufacturer's conditions.

**Cloning of *SATB1* constructs with potential Foxp3 binding regions.**

The corresponding *SATB1* genomic regions were amplified by PCR using human genomic DNA as source material. After digestion the fragments were cloned into the pGL4.24 vector with a minP element upstream of the potential binding motif and a destabilized downstream Firefly luciferase.

Mutated constructs were generated with either PCR-based mutagenesis or the QuikChange Lightning Multi Site-Directed mutagenesis kit (Stratagene) following manufacturer's conditions.

**Luciferase assays.**

To assess regulation of *SATB1* expression by binding of miRNA to the 3'UTR of *SATB1*, constructs were transfected into HEK293T cells in 96-well plates together with miRNA mimics for either miR-155, miR-7, miR-21, miR-34a, miR-18a or a scrambled control miRNA.

To assess regulation of SATB1 expression by binding of Foxp3 to the genomic locus of *SATB1*, constructs were transfected separately into HEK293T cells in 96-well plates together with control plasmid or plasmids expressing Foxp3 as well as a plasmid encoding renilla luciferase for normalization.

Lysis and analysis were performed 24 h post-transfection using the Promega Dual Luciferase Kit. Luciferase activity was counted in a Mithras plate reader (Berthold).

### **Lentiviral vector production.**

High titer lentiviral vector supernatant encoding DsRED T2A SATB1, YFP T2A Foxp3 and control plasmids alone was collected. For silencing of Foxp3 and SATB1 in human T<sub>reg</sub> cells, miR RNAi targeting Foxp3 and SATB1 were designed, cloned into the pcDNA6.2-GW+EmGFP-miR vector, chained and recombined into the pLenti6.3 expression vectors (Invitrogen). For transduction of murine expanded T<sub>reg</sub> cells, SATB1 was cloned into the pLVTHM expression vector in front of an IRES-Thy1.1 sequence<sup>53</sup>.

### **Lentiviral Foxp3 and SATB1 transductions of human CD4<sup>+</sup> T cells.**

Human CD4<sup>+</sup>CD25<sup>+</sup> T<sub>reg</sub> cells were stimulated for 24 h with CD3 and CD28-coated beads in the presence of IL-2. After this initial stimulation, T<sub>reg</sub> cells were lentivirally transduced with a pELNS DsRED 2A SATB1 or control plasmids containing DsRED as previously described resulting in a 1:1 expression of DsRED and the transgene<sup>39</sup>, expanded for 6 days in the presence of CD3 and CD28-coated beads and IL-2, sorted on DsRED-positive cells on a MoFlo sorter (DakoCytomation) and used for further experiments.

**Filter retention analysis.**

Each individual  $^{32}\text{P}$ -radiolabeled dsDNA sequence (14 nM) was incubated with increasing concentrations of Foxp3 protein for 30 min at 37 °C in 25  $\mu\text{l}$  of binding buffer (KCl-Tris, pH 7.6, 5% Glycerol, 3 mM  $\text{MgCl}_2$ , 2 mM DTT) in the presence of 1  $\mu\text{g/ml}$  tRNA (Roche) and 50  $\mu\text{g/ml}$  BSA. After incubation, the binding reaction was filtered through pre-wet 0.45  $\mu\text{m}$  nitrocellulose filter membrane (Millipore) to co-retain protein and bound DNA. Membranes were washed and the amount of bound DNA-protein complexes determined by autoradiography.

**Expansion of mouse  $\text{T}_{\text{reg}}$  cells.**

$\text{CD4}^+\text{CD25}^+\text{GFP}^+$   $\text{T}_{\text{reg}}$  cells were isolated from lymph nodes and spleens of DERE mice. Cells were pre-enriched with the mouse  $\text{CD4}^+$  T cell isolation kit according to manufacturer's instructions (Miltenyi Biotech). Following enrichment, cells were stained with CD4, CD25, CD3, and  $\text{CD8}\alpha$ . Cells were sorted on a FACS Aria III (BD) (purity > 98.0%). Cells were expanded *in vitro* by activation with Dynabead mouse T cell activator CD3+CD28-coated microbeads (3:1 bead to  $\text{T}_{\text{reg}}$  cell ratio, Invitrogen) with exogenous IL-2 (2000 IU/ml, Proleukin) as previously described<sup>54</sup>.

**Lentiviral transductions of mouse  $\text{T}_{\text{reg}}$  cells.**

After expansion for 10 to 14 days in the presence of CD3+CD28-coated beads and IL-2, murine  $\text{T}_{\text{reg}}$  cells were lentivirally transduced with a pLVTHM-SATB1-IRES-Thy1.1 plasmid or control plasmids. Therefore,  $2.5 \times 10^5$  cells per well were transduced in 500  $\mu\text{l}$  total volume of fresh culture media in a 24-well plate containing lentivirus (20 TU/cell) and

protamine sulfate (8 µg/ml; Sigma-Aldrich). Cells were spin-inoculated by centrifugation at  $1000\times g$  for 90 min at 30°C, fresh medium was added and cells were incubated for an additional 2 h at 37 °C. Afterwards, cells were washed several times and cultivated in the presence of CD3+CD28-coated beads and IL-2. Transgene expression was assessed no earlier than 72 h post-transduction. SATB1-Thy1.1-transduced, control-transduced or non-transduced expanded  $T_{reg}$  cells were sorted on GFP and Thy1.1 expression or GFP expression alone on a FACS Aria III (BD) and used for further experiments.

### **Induction and assessment of colitis.**

Splenocyte samples were enriched for  $CD4^+$  T cells by negative selection on MACS columns with the  $CD4^+$  T cell isolation kit II (Miltenyi Biotec). Cells were then stained with CD45RB, CD25, CD4, CD8 $\alpha$ , and CD3 (all from BD) and naïve  $CD4^+CD25^-CD45RB^{hi}$  T cells were sorted on a FACS Aria III. Inflammatory bowel disease was induced by the adoptive transfer of  $6 \times 10^5$  naïve  $CD4^+CD45RB^{hi}$  T cells that were purified from C57BL/6 mice into *Rag2*<sup>-/-</sup> animals by tail vein injection. Mice that received  $1 \times 10^5$  control-transduced expanded  $CD4^+GFP^+$   $T_{reg}$  cells from DEREK mice at the same time as the naïve  $CD4^+CD45RB^{hi}$  T cells served as controls. To test the function of SATB1-expressing  $T_{reg}$  cells, mice received  $1 \times 10^5$  SATB1-transduced expanded  $CD4^+GFP^+$   $T_{reg}$  cells from DEREK mice together with the naïve  $CD4^+CD45RB^{hi}$  T cells. Recipient mice were weighed 3 times per week and monitored for signs of illness. After 9 weeks, the animals were sacrificed, and the mesenteric and peripheral lymph nodes as well as spleen were analyzed by flow cytometry. For histological analysis, the large intestine (from the ileo-ceco-colic junction to the anorectal junction) was removed, fixed in 10% buffered

formalin solution, and routinely processed for histological examination. Sections were stained with hematoxylin and eosin and assigned scores as described<sup>55</sup>. All samples were coded and assigned scores by researchers 'blinded' to the experimental conditions.

### **Statistical analysis.**

Student's *t*-tests and ANOVA with LSD were performed with SPSS 19.0 software.

### **Additional methods.**

More detailed information on mice, reagents, antibodies, plasmids, experimental procedures, and the generation of lentiviral vectors is available in the Supplementary Methods.

## REFERENCES

1. Sakaguchi, S., Yamaguchi, T., Nomura, T. & Ono, M. Regulatory T cells and immune tolerance. *Cell* **133**, 775-787 (2008).
2. Lin, W. *et al.* Regulatory T cell development in the absence of functional Foxp3. *Nat Immunol* **8**, 359-368 (2007).
3. Wan, Y.Y. & Flavell, R.A. Regulatory T-cell functions are subverted and converted owing to attenuated Foxp3 expression. *Nature* **445**, 766-770 (2007).
4. Lahl, K. *et al.* Nonfunctional regulatory T cells and defective control of Th2 cytokine production in natural scurfy mutant mice. *J Immunol* **183**, 5662-5672 (2009).
5. Williams, L.M. & Rudensky, A.Y. Maintenance of the Foxp3-dependent developmental program in mature regulatory T cells requires continued expression of Foxp3. *Nat Immunol* **8**, 277-284 (2007).
6. Fontenot, J.D., Gavin, M.A. & Rudensky, A.Y. Foxp3 programs the development and function of CD4<sup>+</sup>CD25<sup>+</sup> regulatory T cells. *Nat Immunol* **4**, 330-336 (2003).
7. Hori, S., Nomura, T. & Sakaguchi, S. Control of regulatory T cell development by the transcription factor Foxp3. *Science* **299**, 1057-1061 (2003).
8. O'Shea, J.J. & Paul, W.E. Mechanisms underlying lineage commitment and plasticity of helper CD4<sup>+</sup> T cells. *Science* **327**, 1098-1102 (2010).
9. Murphy, K.M. & Stockinger, B. Effector T cell plasticity: flexibility in the face of changing circumstances. *Nat Immunol* **11**, 674-680 (2010).
10. Feuerer, M., Hill, J.A., Mathis, D. & Benoist, C. Foxp3<sup>+</sup> regulatory T cells: differentiation, specification, subphenotypes. *Nat Immunol* **10**, 689-695 (2009).

11. Lee, Y.K., Mukasa, R., Hatton, R.D. & Weaver, C.T. Developmental plasticity of Th17 and Treg cells. *Curr Opin Immunol* **21**, 274-280 (2009).
12. Gavin, M.A. *et al.* Foxp3-dependent programme of regulatory T-cell differentiation. *Nature* **445**, 771-775 (2007).
13. Pan, F. *et al.* Eos mediates Foxp3-dependent gene silencing in CD4<sup>+</sup> regulatory T cells. *Science* **325**, 1142-1146 (2009).
14. Ouyang, W. *et al.* Foxo proteins cooperatively control the differentiation of Foxp3<sup>+</sup> regulatory T cells. *Nat Immunol* **11**, 618-627 (2010).
15. Harada, Y. *et al.* Transcription factors Foxo3a and Foxo1 couple the E3 ligase Cbl-b to the induction of Foxp3 expression in induced regulatory T cells. *J Exp Med* **207**, 1381-1391 (2010).
16. Zheng, Y. *et al.* Regulatory T-cell suppressor program co-opts transcription factor IRF4 to control T(H)2 responses. *Nature* **458**, 351-356 (2009).
17. Chaudhry, A. *et al.* CD4<sup>+</sup> regulatory T cells control TH17 responses in a Stat3-dependent manner. *Science* **326**, 986-991 (2009).
18. Ziegler, S.F. FOXP3: of mice and men. *Annu Rev Immunol* **24**, 209-226 (2006).
19. Chong, M.M., Rasmussen, J.P., Rudensky, A.Y. & Littman, D.R. The RNaseIII enzyme Droscha is critical in T cells for preventing lethal inflammatory disease. *J Exp Med* **205**, 2005-2017 (2008).
20. Liston, A., Lu, L.F., O'Carroll, D., Tarakhovsky, A. & Rudensky, A.Y. Dicer-dependent microRNA pathway safeguards regulatory T cell function. *J Exp Med* **205**, 1993-2004 (2008).

21. Zhou, X. *et al.* Selective miRNA disruption in T reg cells leads to uncontrolled autoimmunity. *J Exp Med* **205**, 1983-1991 (2008).
22. Floess, S. *et al.* Epigenetic control of the foxp3 locus in regulatory T cells. *PLoS Biol* **5**, e38 (2007).
23. Li, B. *et al.* FOXP3 interactions with histone acetyltransferase and class II histone deacetylases are required for repression. *Proc Natl Acad Sci U S A* **104**, 4571-4576 (2007).
24. Zhou, X., Bailey-Bucktrout, S., Jeker, L.T. & Bluestone, J.A. Plasticity of CD4(+) FoxP3(+) T cells. *Curr Opin Immunol* **21**, 281-285 (2009).
25. Alvarez, J.D. *et al.* The MAR-binding protein SATB1 orchestrates temporal and spatial expression of multiple genes during T-cell development. *Genes Dev* **14**, 521-535 (2000).
26. Cai, S., Han, H.J. & Kohwi-Shigematsu, T. Tissue-specific nuclear architecture and gene expression regulated by SATB1. *Nat Genet* **34**, 42-51 (2003).
27. Yasui, D., Miyano, M., Cai, S., Varga-Weisz, P. & Kohwi-Shigematsu, T. SATB1 targets chromatin remodelling to regulate genes over long distances. *Nature* **419**, 641-645 (2002).
28. Dickinson, L.A., Joh, T., Kohwi, Y. & Kohwi-Shigematsu, T. A tissue-specific MAR/SAR DNA-binding protein with unusual binding site recognition. *Cell* **70**, 631-645 (1992).
29. Cai, S., Lee, C.C. & Kohwi-Shigematsu, T. SATB1 packages densely looped, transcriptionally active chromatin for coordinated expression of cytokine genes. *Nat Genet* **38**, 1278-1288 (2006).

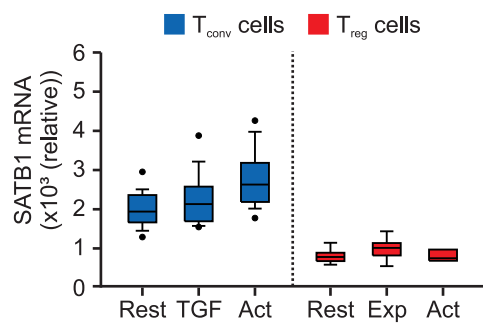
30. Pfoertner, S. *et al.* Signatures of human regulatory T cells: an encounter with old friends and new players. *Genome Biol* **7**, R54 (2006).
31. Zheng, Y. *et al.* Genome-wide analysis of Foxp3 target genes in developing and mature regulatory T cells. *Nature* **445**, 936-940 (2007).
32. Sugimoto, N. *et al.* Foxp3-dependent and -independent molecules specific for CD25+CD4+ natural regulatory T cells revealed by DNA microarray analysis. *Int Immunol* **18**, 1197-1209 (2006).
33. Lund, R. *et al.* Identification of genes involved in the initiation of human Th1 or Th2 cell commitment. *Eur J Immunol* **35**, 3307-3319 (2005).
34. Chen, W. *et al.* Conversion of peripheral CD4+CD25- naive T cells to CD4+CD25+ regulatory T cells by TGF-beta induction of transcription factor Foxp3. *J Exp Med* **198**, 1875-1886 (2003).
35. Lahl, K. *et al.* Selective depletion of Foxp3+ regulatory T cells induces a scurfy-like disease. *J Exp Med* **204**, 57-63 (2007).
36. Anz, D. *et al.* Immunostimulatory RNA Blocks Suppression by Regulatory T Cells. *J Immunol* **184**, 939-946.
37. Kuczma, M. *et al.* Foxp3-deficient regulatory T cells do not revert into conventional effector CD4+ T cells but constitute a unique cell subset. *J Immunol* **183**, 3731-3741 (2009).
38. Ishihara, Y., Ito, F. & Shimamoto, N. Increased expression of c-Fos by extracellular signal-regulated kinase activation under sustained oxidative stress elicits BimEL upregulation and hepatocyte apoptosis. *Febs J* **278**, 1873-1881 (2011).

39. Szymczak, A.L. *et al.* Correction of multi-gene deficiency in vivo using a single 'self-cleaving' 2A peptide-based retroviral vector. *Nat Biotechnol* **22**, 589-594 (2004).
40. Wei, G. *et al.* Global mapping of H3K4me3 and H3K27me3 reveals specificity and plasticity in lineage fate determination of differentiating CD4<sup>+</sup> T cells. *Immunity* **30**, 155-167 (2009).
41. Lu, L.F. *et al.* Foxp3-dependent microRNA155 confers competitive fitness to regulatory T cells by targeting SOCS1 protein. *Immunity* **30**, 80-91 (2009).
42. Kohlhaas, S. *et al.* Cutting edge: the Foxp3 target miR-155 contributes to the development of regulatory T cells. *J Immunol* **182**, 2578-2582 (2009).
43. Marson, A. *et al.* Foxp3 occupancy and regulation of key target genes during T-cell stimulation. *Nature* **445**, 931-935 (2007).
44. Kito, A. *et al.* Indispensable role of the Runx1-Cbfbeta transcription complex for in vivo-suppressive function of FoxP3<sup>+</sup> regulatory T cells. *Immunity* **31**, 609-620 (2009).
45. Rudra, D. *et al.* Runx-CBFBeta complexes control expression of the transcription factor Foxp3 in regulatory T cells. *Nat Immunol* **10**, 1170-1177 (2009).
46. Ahlfors, H. *et al.* SATB1 dictates expression of multiple genes including IL-5 involved in human T helper cell differentiation. *Blood* **116**, 1443-1453 (2010).
47. Koch, M.A. *et al.* The transcription factor T-bet controls regulatory T cell homeostasis and function during type 1 inflammation. *Nat Immunol* **10**, 595-602 (2009).

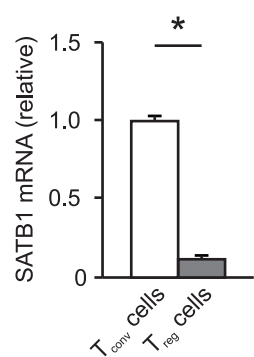
48. Zhou, X. *et al.* Instability of the transcription factor Foxp3 leads to the generation of pathogenic memory T cells in vivo. *Nat Immunol* **10**, 1000-1007 (2009).
49. Oldenhove, G. *et al.* Decrease of Foxp3<sup>+</sup> Treg cell number and acquisition of effector cell phenotype during lethal infection. *Immunity* **31**, 772-786 (2009).
50. Brunkow, M.E. *et al.* Disruption of a new forkhead/winged-helix protein, scurf, results in the fatal lymphoproliferative disorder of the scurfy mouse. *Nat Genet* **27**, 68-73 (2001).
51. Classen, S. *et al.* Human resting CD4<sup>+</sup> T cells are constitutively inhibited by TGFβ under steady-state conditions. *J Immunol* **178**, 6931-6940 (2007).
52. Sadlon, T.J. *et al.* Genome-wide identification of human FOXP3 target genes in natural regulatory T cells. *Journal of immunology* **185**, 1071-1081 (2010).
53. Wiznerowicz, M. & Trono, D. Conditional suppression of cellular genes: lentivirus vector-mediated drug-inducible RNA interference. *Journal of virology* **77**, 8957-8961 (2003).
54. Tang, Q. *et al.* In vitro-expanded antigen-specific regulatory T cells suppress autoimmune diabetes. *The Journal of experimental medicine* **199**, 1455-1465 (2004).
55. ten Hove, T. *et al.* Dichotomous role of inhibition of p38 MAPK with SB 203580 in experimental colitis. *Gut* **50**, 507-512 (2002).

# Figure 1

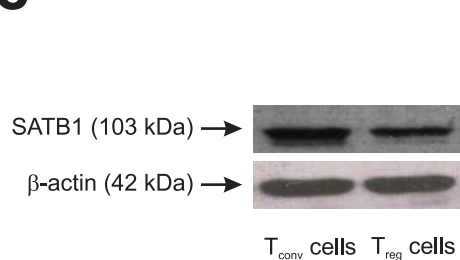
**a**



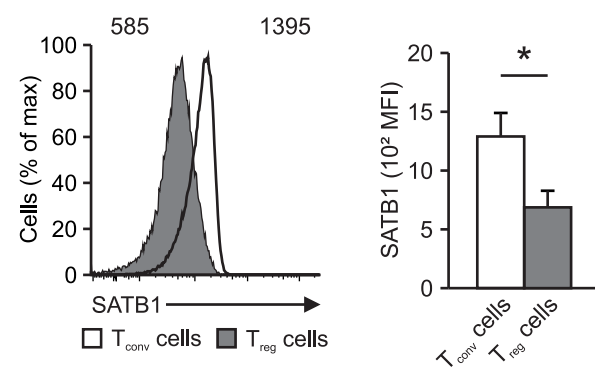
**b**



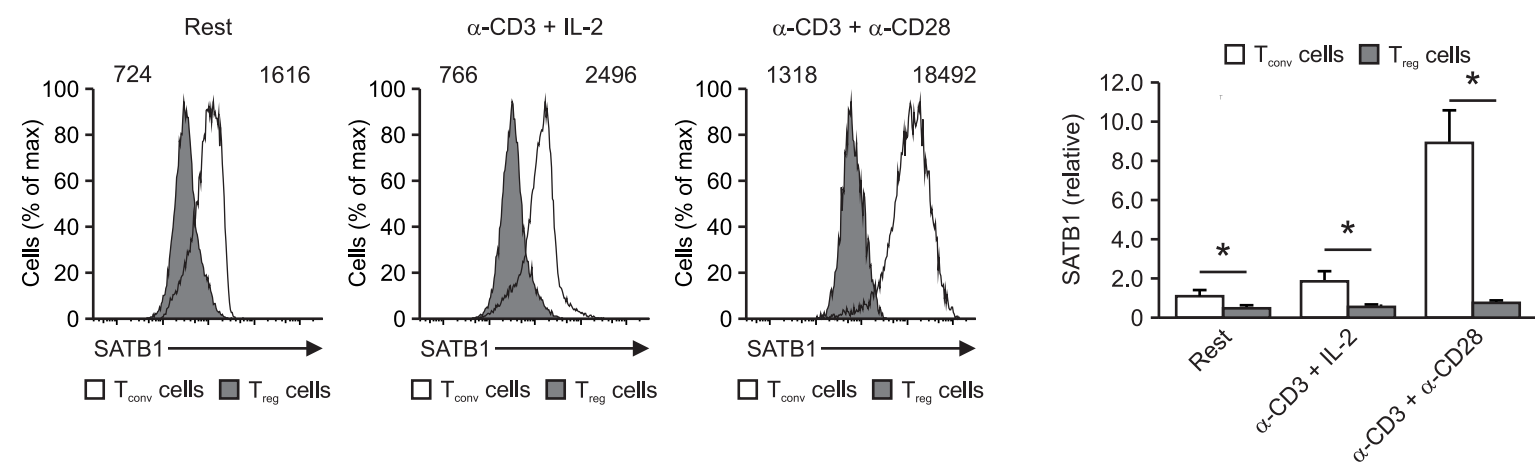
**c**



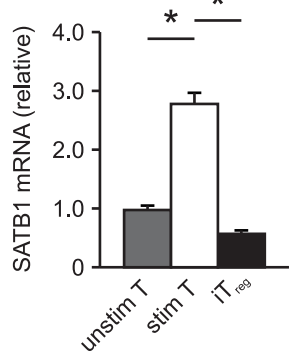
**d**



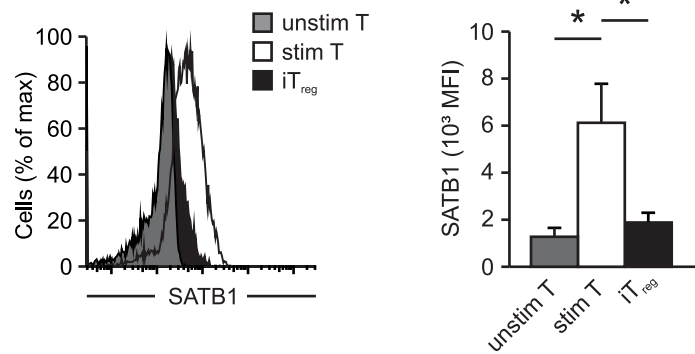
**e**



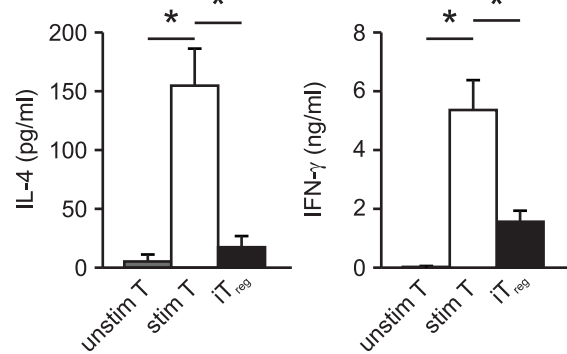
**f**



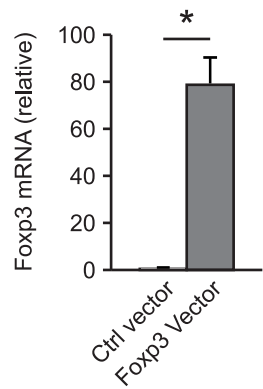
**g**



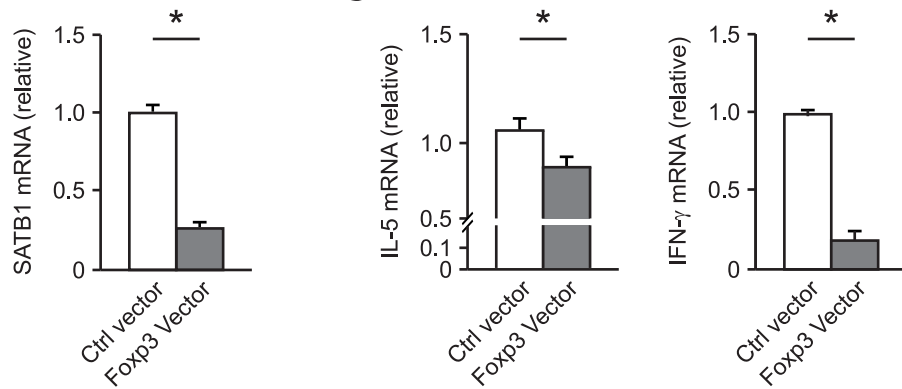
**h**

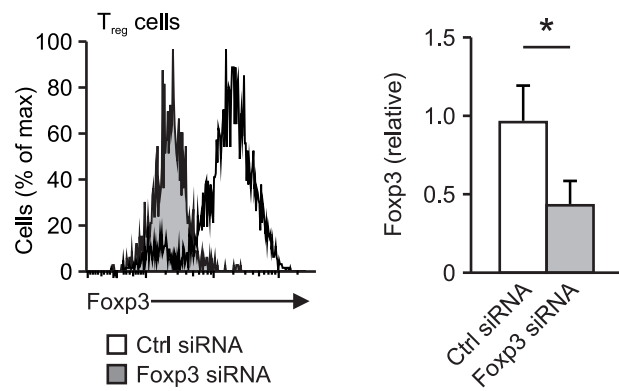
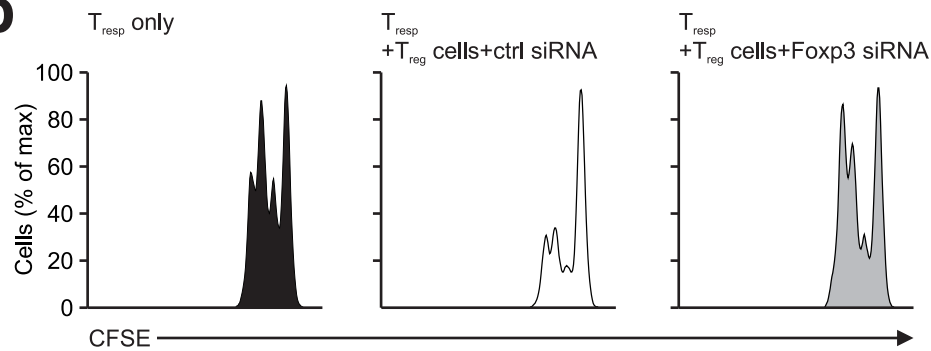
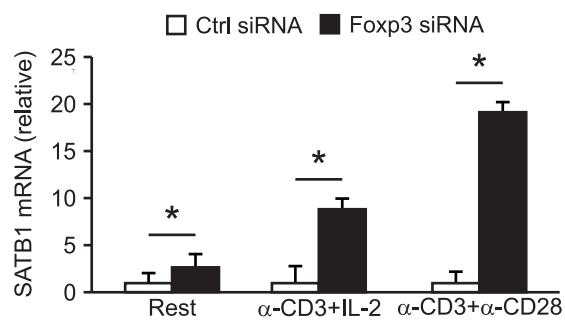
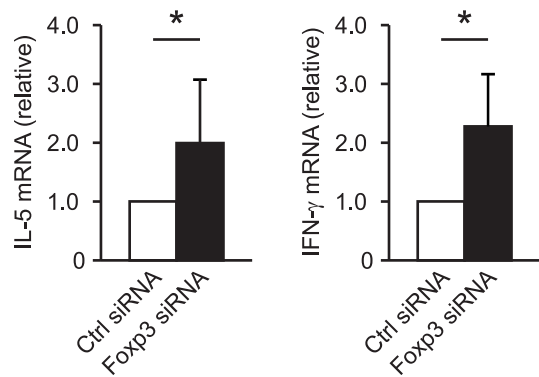
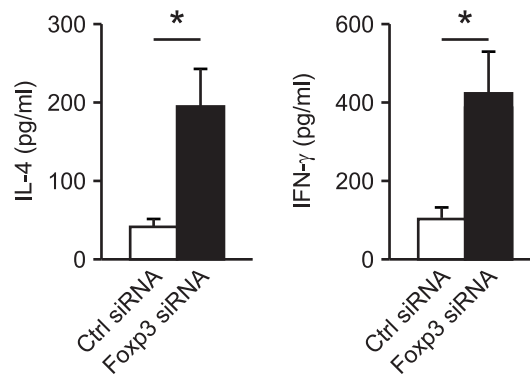
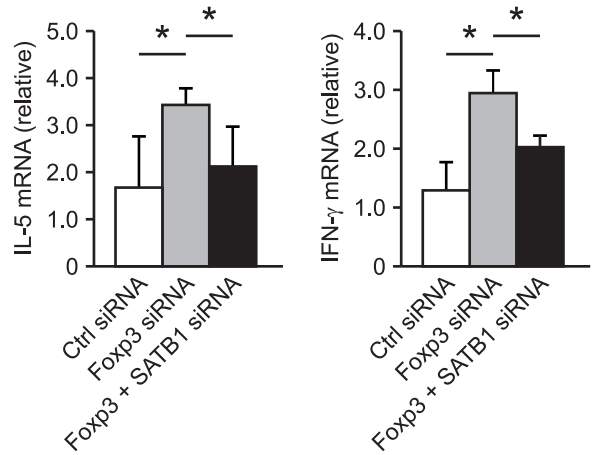


**i**



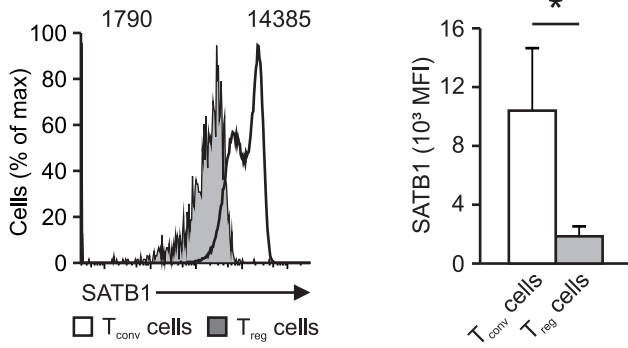
**j**



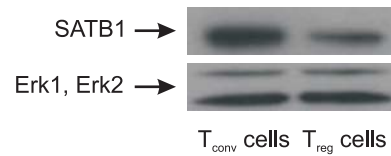
**Fig. 2****a****b****c****d****e****f**

# Fig. 3

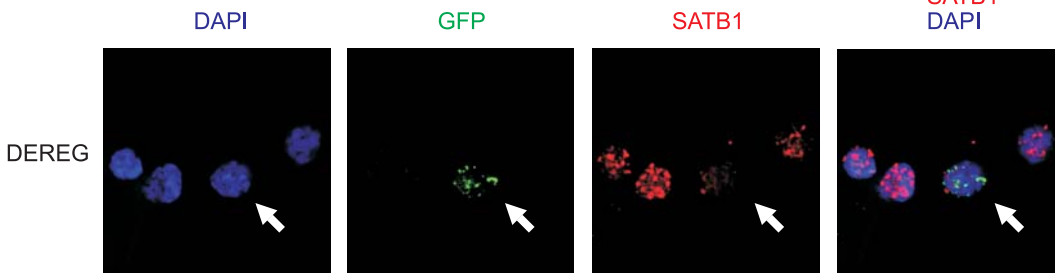
**a**



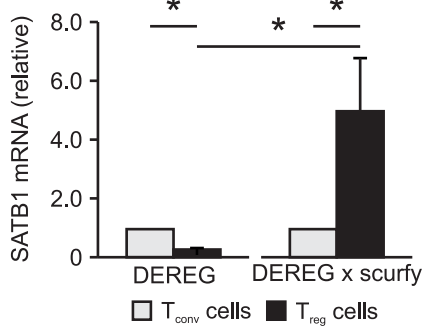
**b**



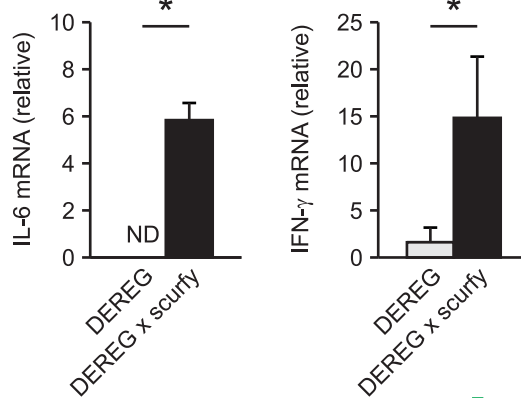
**c**



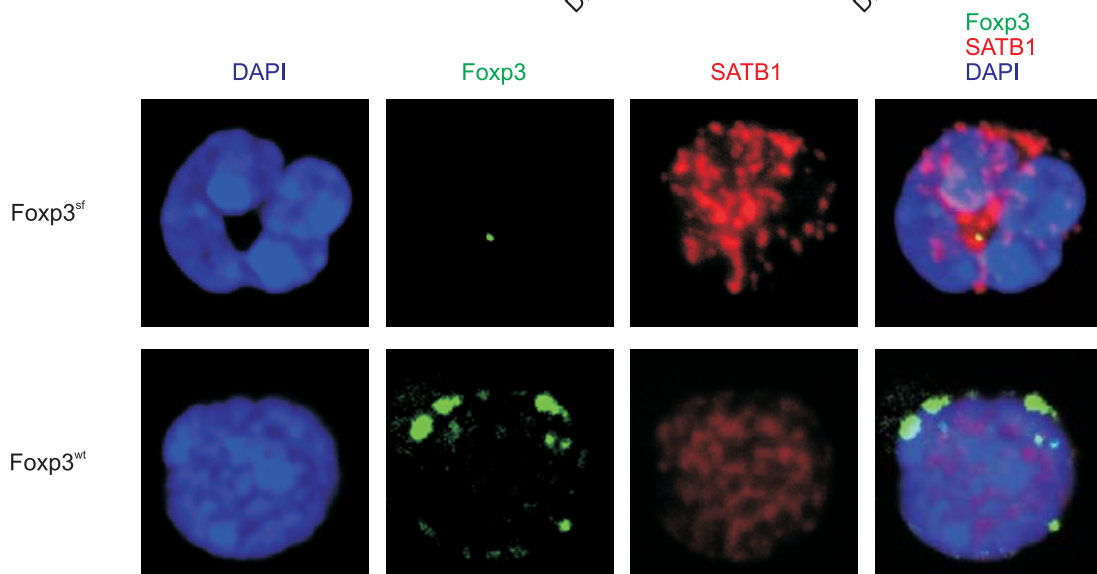
**d**



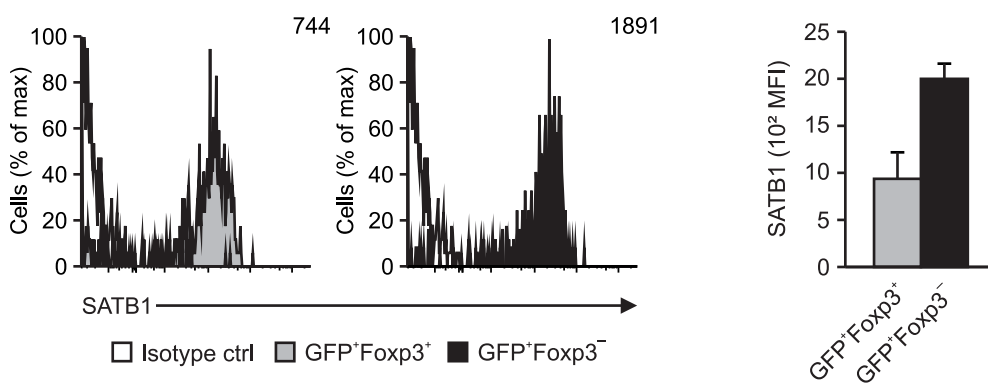
**e**

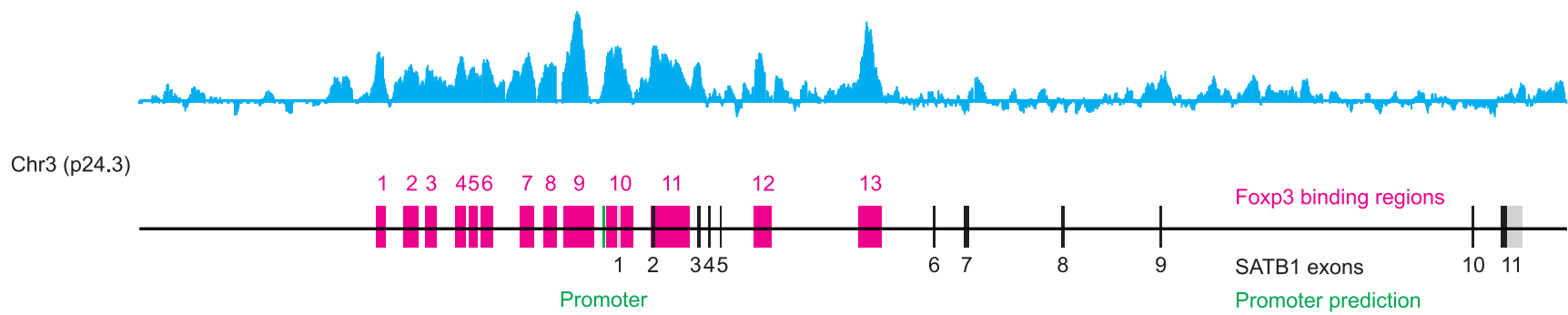
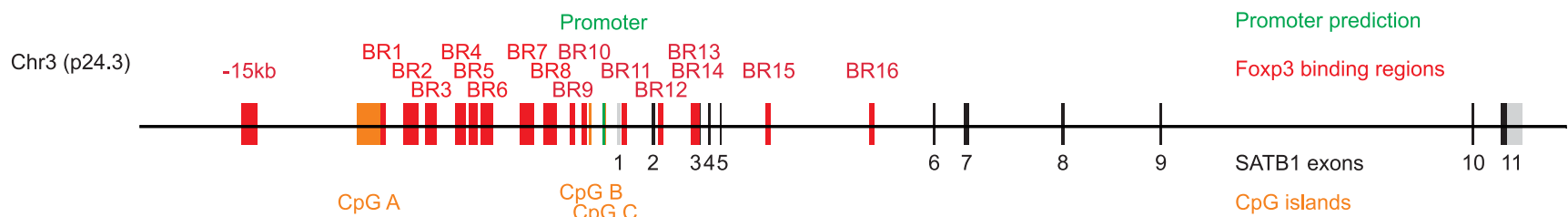
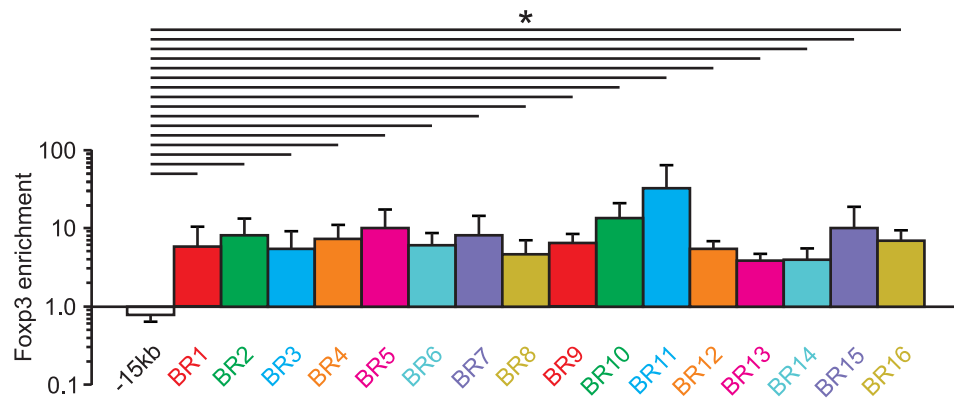
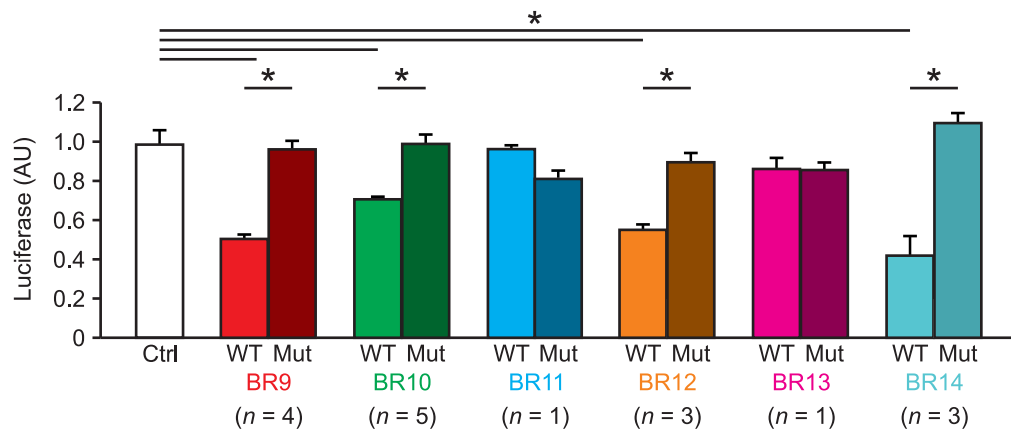
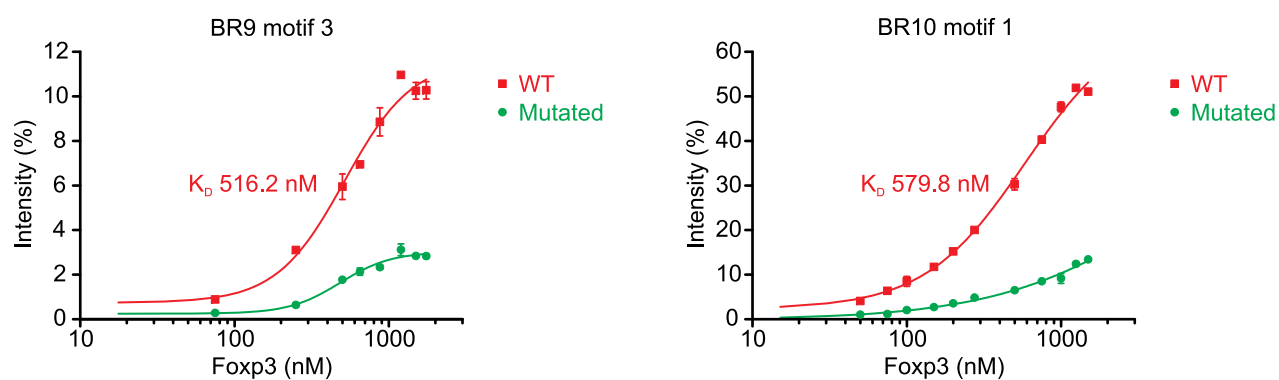


**f**

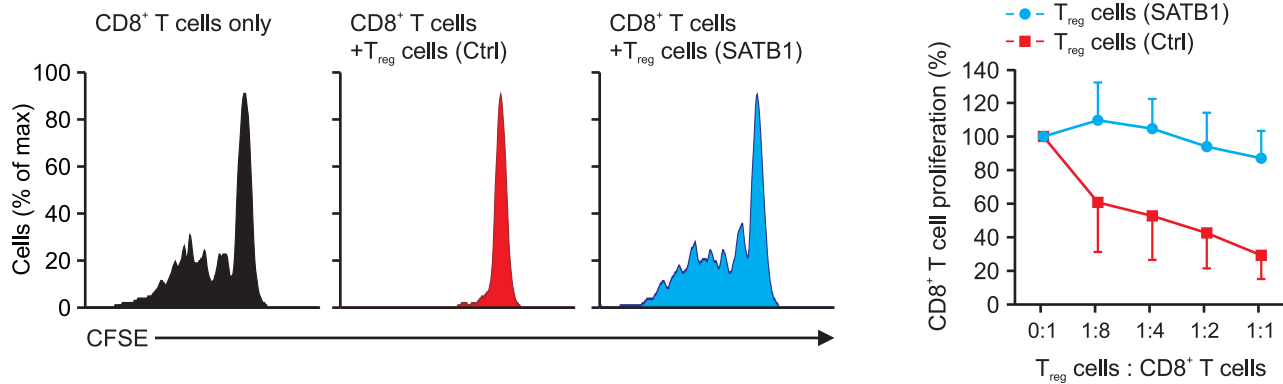
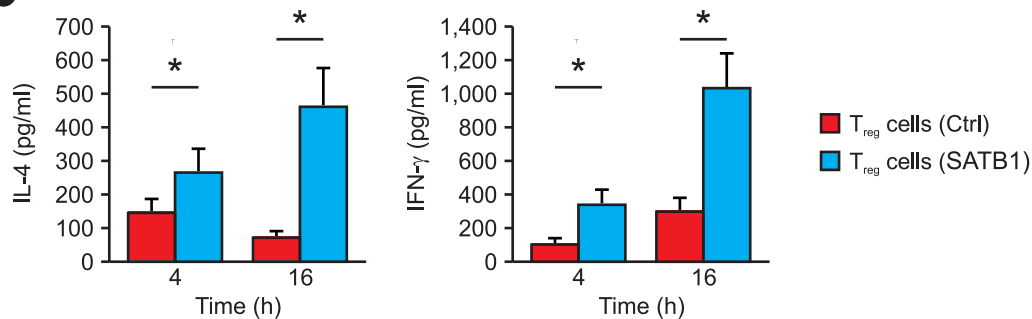
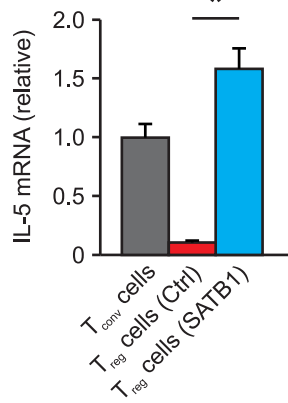
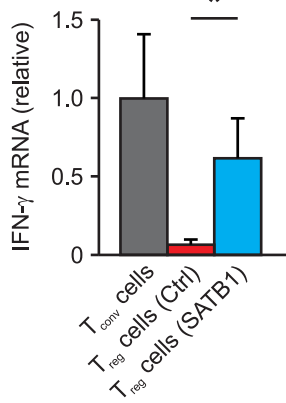
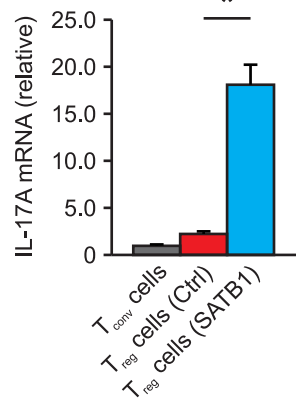


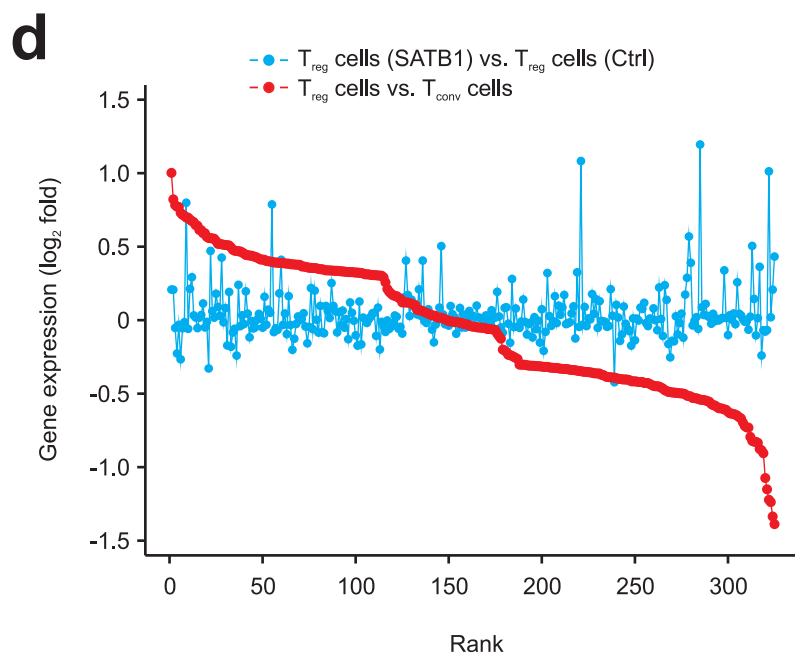
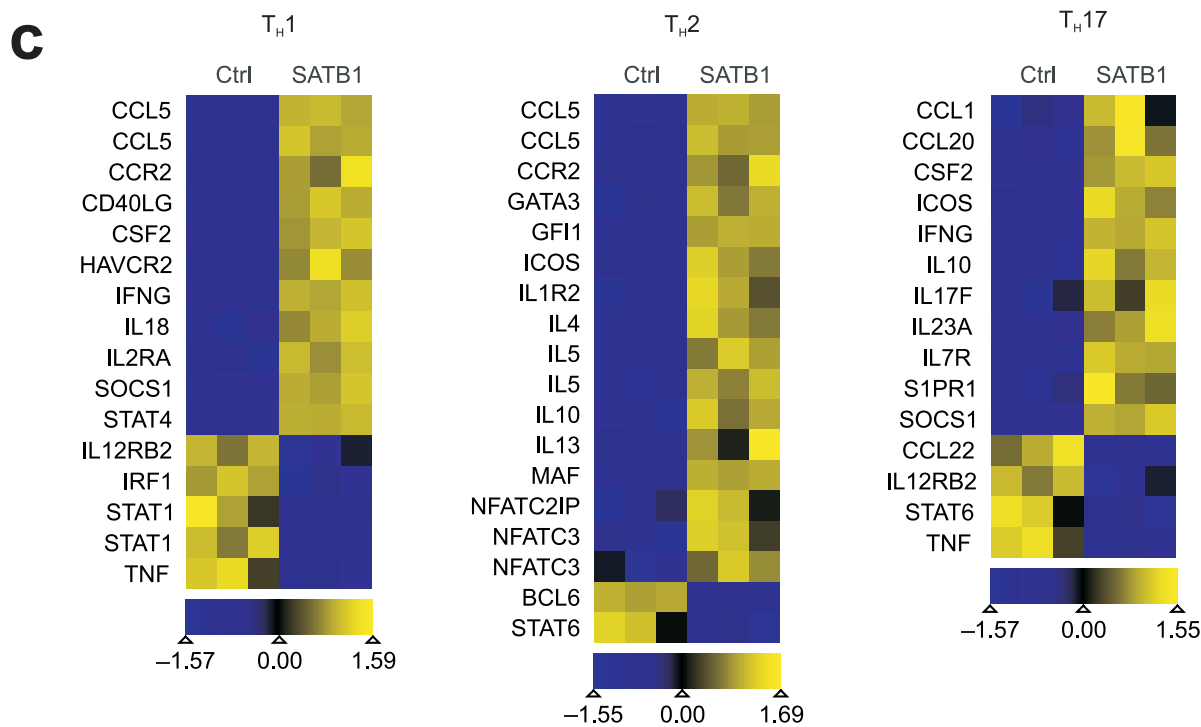
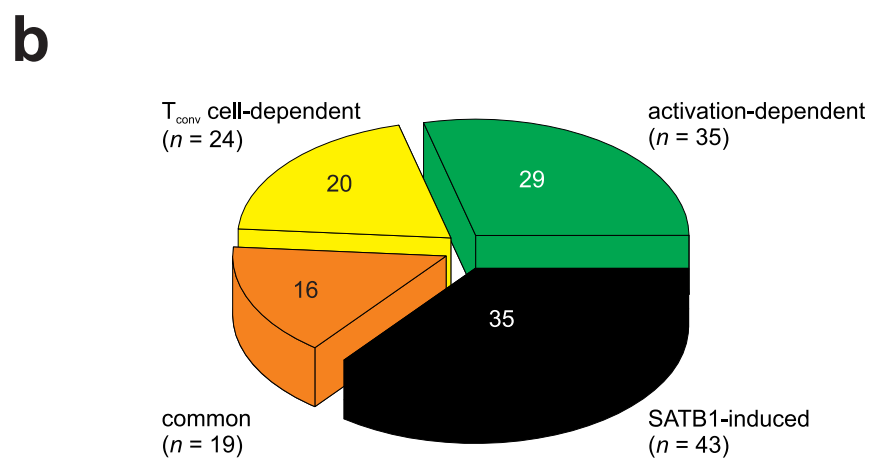
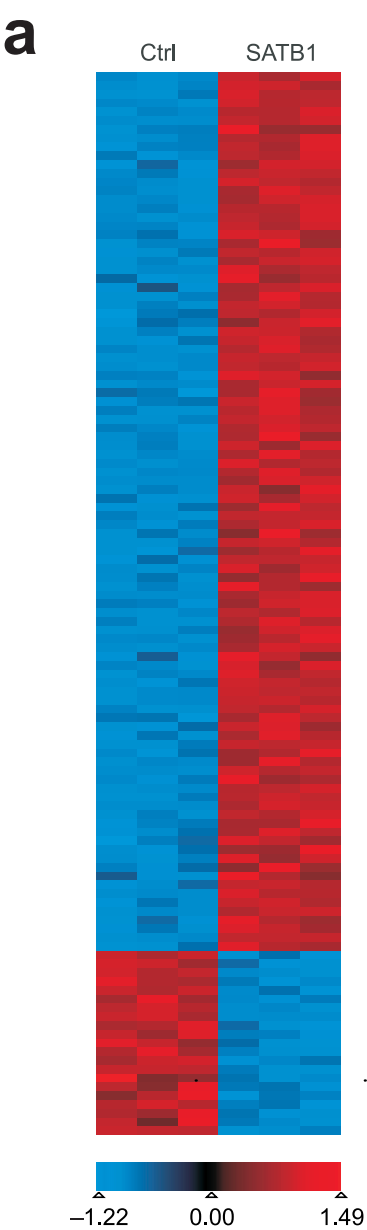
**g**

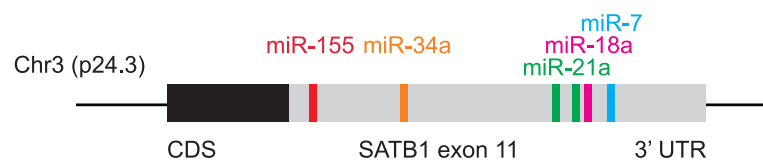
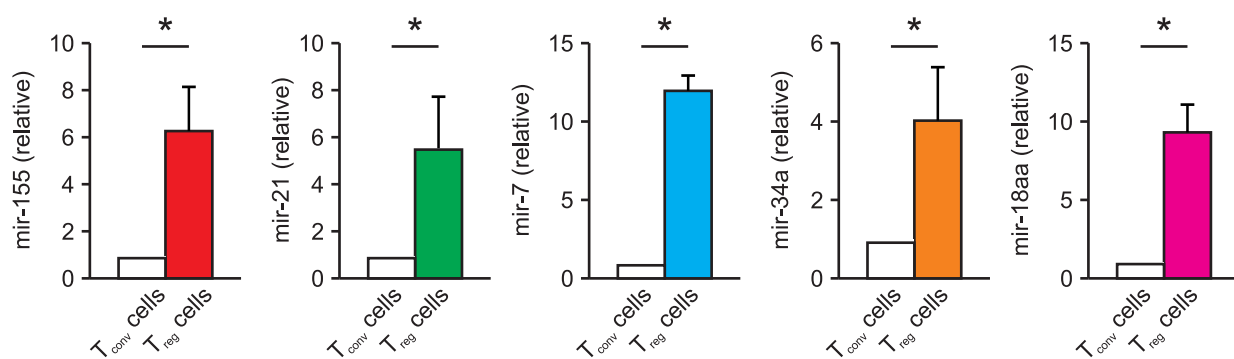
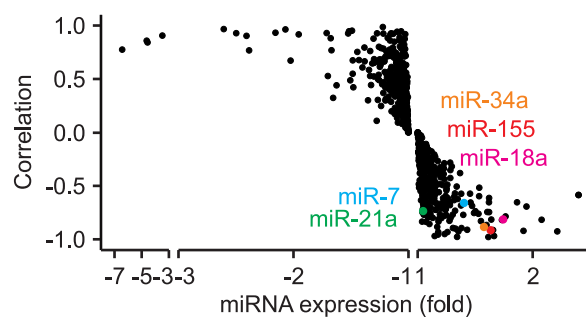
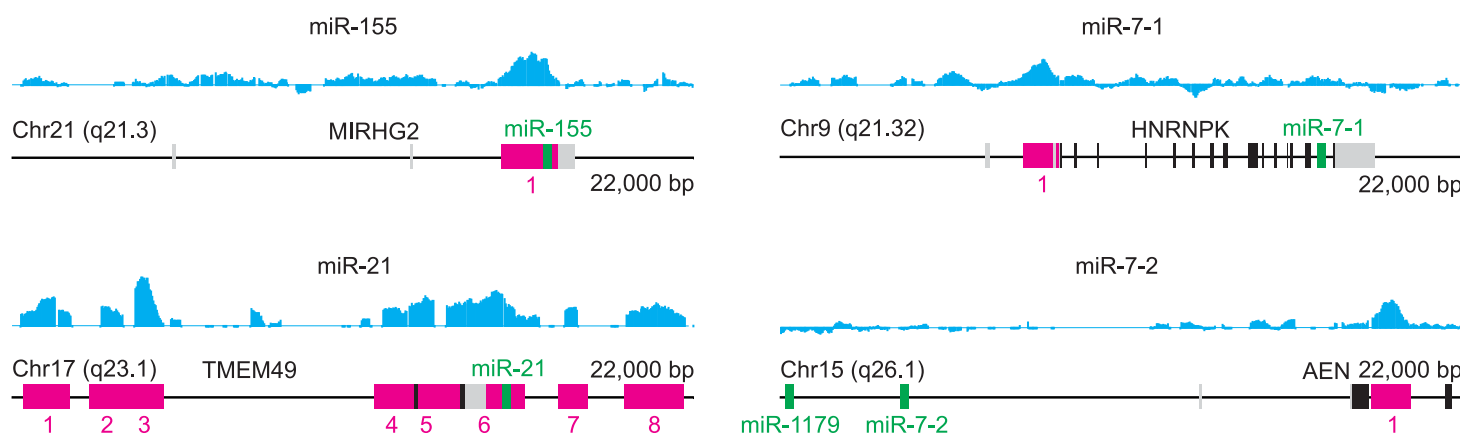
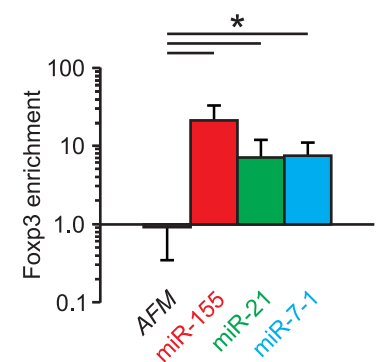
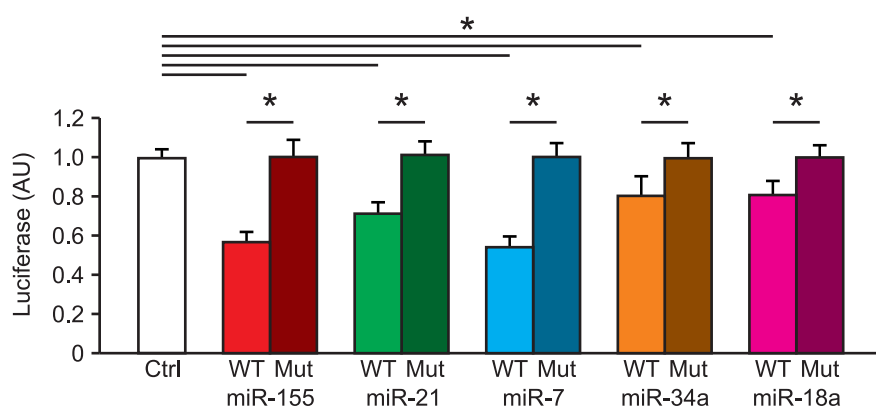
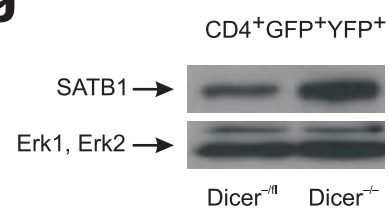


**Fig. 4****a****b****c****d****e**

# Fig. 5

**a****b****c****d****e**

**Fig. 6**

**Fig. 7****a****b****c****d****e****f****g**

# Fig. 8

